ACCELERATOR PHYSICS REQUIREMENTS FOR ELECTRON COOLER AT THE EIC INJECTION ENERGY*

A.V. Fedotov#, D. Kayran, S. Seletskiy
Brookhaven National Laboratory, Upton, NY, U.S.A.

Abstract

An electron cooler using RF-accelerated electron beam is presently under design to provide required cooling of protons at the EIC injection energy of 24 GeV. In this paper, we describe accelerator physics requirements and design considerations of such 13 MeV electron cooler, including associated challenges.

INTRODUCTION

The Electron-Ion Collider (EIC) is a partnership project between Brookhaven National Laboratory (BNL) and Thomas Jefferson National Accelerator Facility (TJNAF) to be constructed at BNL, using much of the existing infrastructure of the Relativistic Heavy Ion Collider (RHIC); a layout of the EIC is shown in Fig. 1. Collisions occur between the hadrons in the Hadron Storage Ring (HSR) and the electrons supplied by the Electron Storage Ring (ESR); in order to maintain a high average polarization of the ESR, bunches are frequently replaced using the Rapid Cycling Synchrotron (RCS) [1].

In order to achieve the design emittances of the hadron beam, hadron beams are injected into the HSR and precooled to the target emittances at injection energy of protons of 24 GeV. After the target emittances are achieved, the HSR is ramped to the collision energy, and the hadron beam is cooled during collision using high-energy cooling system. Several options of such high-energy cooling system, based on Coherent Electron Cooling (CeC) [2, 3] and on Electron Cooling using storage ring [4-6], are being considered.

Precooling of protons at 24 GeV will be done using conventional electron cooling technique which requires 13 MeV electron accelerator. The design of such a Precooler is based on RF-accelerated electron bunches, similar to LEReC [7], but scaled to higher energy. The Precooler energy can be extended to 22 MeV to provide cooling of protons at collision energy of 41 GeV.

COOLER REQUIREMENTS

The Precooler design is based on the non-magnetized cooling approach with zero magnetic field on the cathode and no magnetic field in the cooling region [7].

The friction force acting on the ion with charge number Z inside a non-magnetized electron beam with velocity distribution function $f(v_e)$ is

$$\vec{F} = -\frac{4\pi n_e e^4 Z^2}{m} \int \ln\left(\frac{\rho_{max}}{\rho_{min}}\right) \frac{\vec{V}_i - \vec{v}_e}{\left|\vec{V}_i - \vec{v}_e\right|^3} f(v_e) d^3 v_e, (1)$$

where e and m are the electron charge and mass, V and v_e are the ion and electron velocities respectively, and n_e is electron density in the particle rest frame (PRF).
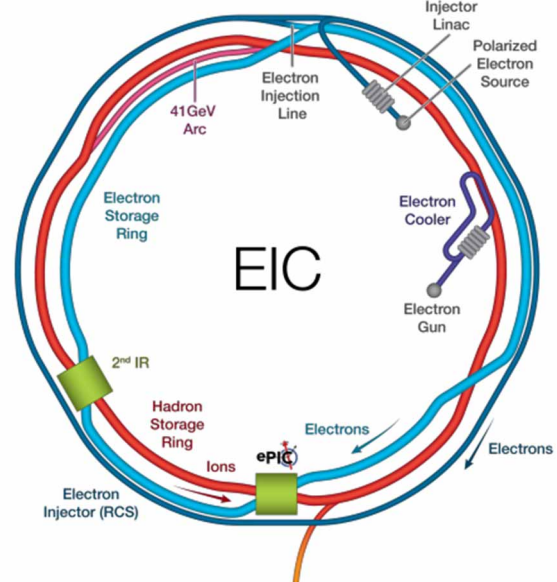
Figure 1: The layout of the Electron-Ion Collider (EIC). The Hadron Storage Ring (HSR), Electron Storage Ring (ESR), and the Rapid Cycling Synchrotron (RCS) labels are color-coded to their respective rings; the current and proposed IRs are shown at IR6 and IR8, with both Precooler and high-energy cooling systems located in IR2.

As cooling of protons (Z=1) is the most challenging task compared to cooling of heavy ions, in this report we focus on cooler parameters considering only proton beams.

To maximize the cooling power and to preserve transverse distribution of hadrons under cooling, the electron beam rms velocity spreads are chosen close to those of the hadron beam. At injection energy in the EIC with $\gamma=25.4$, the proton beam with bunch intensities $N=2.8\times10^{11}$ will have rms longitudinal momentum spread of about $\sigma_p=5\text{-}6\times10^{-4}$. This sets the requirement for the rms momentum spread of electron beam $< 5\times10^{-4}$. For the rms normalized emittance of the proton beam around 2 μm and 200 m beta function in the cooling section, the hadron beam rms angular spread in the lab frame is 0.02 mrad. This gives the requirement for the electrons angular spread θ in the cooling section around 0.02 mrad (as presented in Table 1).

MOPAM2R1

SPECIFICATIONS AND STATUS OF THE NEW ELECTRON COOLER FOR THE CERN ANTIPROTON DECELERATOR (AD)

A. Rossi*, C. Accettura, W. Andreazza, A. Bollazzi, C. Castro Sequeiro, J. Cenede,
N. Chritin, Y. Coutron, A. Frassier, G. Khatri, D. Gamba, L. Joergensen, C. Machado,
O. Marqversen, L. Ponce, A. Pikin, J. A. Ferreira Somoza, M. Sameed, Y. Thurel,
A. Sinturel, T. Todorcevic, G. Tranquille, L. von Freeden, CERN, Geneva, Switzerland

Abstract

A new electron cooler for the Antiproton Decelerator (AD) is being designed at CERN, and will replace the current device (in operation for more than 40 years), during the next Long Shutdown (2026-2028). The functional specifications, recalled in this paper, favour high reliability, with improved performance in terms of time of cooling, obtained mainly with better field quality and possibly higher electron beam current. The status of the new electron cooler design is presented, showing an evolution that aims at easing integration, installation and maintenance.

INTRODUCTION

The AD (Antiproton Decelerator) ring decelerates antiprotons ($\bar{p}$) from 3.5 GeV/c to 100 MeV/c which are then injected into the ELENA (Extra Low ENergy Antiproton) ring. To counteract beam blow up during deceleration, stochastic cooling and electron cooling are carried out during the AD cycle, with electron cooling operating at 300 and 100 MeV/c momentum of the circulating beam [1]. While the AD ring has been operating since the year 2000, the current electron cooler is around 40 years old, being recovered from the Low Energy Antiproton Ring (1982-1997) [2]. The magnets are even older and the companies who produced them no longer exist. A replacement for the electron cooler is therefore envisaged, in the frame of the Consolidation Project at CERN. The new device aims at a high reliability, by design and robustness of the ancillary equipment. Moreover, it is expected to have improved performance in terms of time of cooling, mainly obtained by limiting the electron transverse and longitudinal temperature and switching on/off the electron beam during the energy ramps, as described in the following. In this paper we give the main parameters of design of the new cooler, explaining the technical choices implemented as an evolution of what was presented in [3]. A brief overview of planning for installation will also be given.

SPECIFICATIONS FOR THE NEW ELECTRON COOLER

The specifications [4] for the new electron cooler are listed in Table 1 where the main design parameters are compared to the one of the presently installed electron cooler, with blue font highlighting the main differences. The cooling will act at the same momentum plateaux as for the current AD cycle,

* adriana.rossi@cern.ch

Table 1: Main Parameters of the Present and New E-Cooler

	Present	**This Spec.**
Gun:		
Magnetic field [T]	0.06	0.24 †
Perveance [$\mu A V^{2/3}$]	0.58	2.5
Cathode radius [mm]	25	12.5
Toroid:		
Magnetic field [T]	0.06	0.06
Angle ϕ_0 [rad]	0.6283	0.6283
Radius r_{tor} [m]	1.133	1.133
Integrated $\perp$ field [T·m]	~ 0.016	$\lesssim$ 0.016
Cooling region:		
Vacuum pressure [mbar]	~ 10^{-10}	< 10^{-10}
Length [m]	< 1	~ 1
Radius [mm]	25	$\geq$ 25
Magnetic field [T]	0.06	0.06
$(B_\perp/B_\parallel)_{max}$	10^{-3}	10^{-4}
$(B_\perp/B_\parallel)_{rms}$	n.a.	< 10^{-4}
e^- $k_B T_\perp$ [meV]	100	$\lesssim$ 100
e^- $k_B T_\parallel$ [meV]	—	$\lesssim$ 1
$r_{e\text{-beam}}$ [mm]	—	up to 25
E_{e^-} [keV]	2.9 $_{100\,MeV/c}$ 25.5 $_{300\,MeV/c}$	2.9 $_{100\,MeV/c}$ 25.5 $_{300\,MeV/c}$
E_{e^-} resolution [eV]	1	0.1 $_{2.9\,keV}$ 1 $_{25.5\,keV}$
E_{e^-} stability [eV]	—	< 0.1 $_{2.9\,keV}$ < 1 $_{25.5\,keV}$
e^- current I_0 [A]	2.4	2.4 $_{nominal}$ 4.8 $_{ultimate}$
Stability [$\Delta I/I_0$]	—	~ 10^{-4}
Relative losses [$\delta I/I_0$]	—	< 10^{-4}
Max time to vary from 25.5 keV to 2.9 keV [s]	> 5	~ 1
e^- beam start/stop [s]	—	$\ll$ 1
BPM relative $e^-/\bar{p}$ accuracy [μm]	—	$\lesssim$ 100
E-cooler availability	—	99%

† The main differences are highlighted in blue in the text

i.e. 300 and 100 MeV/c momentum of the circulating beam. In designing the new electron cooler, we tried to improve its performance and reduce the time of cooling, as well as guarantee good reliability. This is approached by trying to limit the transverse and longitudinal electron velocity

DYNAMIC APERTURE AND FREQUENCY ANALYSIS IN ELENA WITH ELECTRON COOLER MAGNETIC FIELD INCLUDED

Lajos Bojtár, CERN Beams Departement

Abstract

We present a new tracking algorithm and its implementation called SIMPA. It has the unique feature of long-term tracking of charged particles in arbitrary static electromagnetic fields in a symplectic way. It is relevant to beam dynamics and optics studies whenever the usual hard-edge model cannot describe the accelerator elements accurately or the beamline contains complex magnetic or electric fields. Such a situation arises in the ELENA machine at CERN and many other rings containing an electron cooler. The magnetic field of the electron cooler has a significant influence on the beam dynamics. Frequency analysis and dynamics aperture studies in ELENA are presented with the electron cooler magnetic field included.

INTRODUCTION

Long-term tracking of charged particles is a fundamental problem of accelerator physics, plasma physics, and it is important in astrophysics. In earlier papers [1, 2] we described a new algorithm allowing long-term symplectic integration of charged particle trajectories in arbitrary static magnetic and electric fields. The approach to particle tracking we described naturally includes the end fields for all kinds of magnets and special elements, like the magnetic system of an electron cooler, with the same treatment. The aim of this paper is to introduce the SIMPA algorithm and software [3] to the cooling expert community. The beam dynamics studies made on the Extra Low ENergy Antiproton (ELENA) ring [4] with SIMPA can be applied to other rings.

THE SIMPA ALGORITHM

We recommend reading the previous papers [1, 2] to understand the algorithm in detail, as only a summary is provided here.

Symplectic integrators keep the conserved quantities bounded, but cannot cure the errors coming from the representation of the fields. These are two separate sources of errors. It is crucial to have a physically valid representation of the fields obeying Maxwell's equations close to machine precision, otherwise there is a spurious energy drift during the tracking. This requires a continuous description of the electromagnetic fields in the entire beam region without any cuts. This is an important difference between SIMPA and other tracking codes which usually make element by element tracking and do not handle the electromagnetic field of the ring or beam line as a whole.

The Modified Surface Method

Surface methods describe the fields on the boundary surrounding the region of interest. Field values on the surface

determine the magnetic or electric fields in a source-free region. This is true because these fields are harmonic functions satisfying the Laplace equation which has a unique solution for a given boundary condition.

As a first step, the potentials are expressed analytically in terms of point sources. Sources are placed outside the volume of interest, at some distance above the boundary, and their strength is calculated by a system of linear equations such that they reproduce the magnetic or electric field at the boundary. In case of a static electric field, electric point sources are used, since the normal component of the field on the boundary surface is sufficient to describe the field inside the volume. For a static magnetic field this is not always true [1]. For example a field of a solenoid coil can not be reproduced by magnetic monopoles. In early versions of SIMPA, additionally to the magnetic monopoles, current loops were also used. This approach however has several drawbacks. Dirac's magnetic monopoles has singularities which must be directed such, that they do not intersect the volume of interest. The Dirac string singularities also prevent using the Fast Multipole Method [5] for the calculation of field maps. For these reasons the magnetic monopoles recently has been replaced by current point sources. These are two infinitesimally small wires perpendicular to each other and parallel to the boundary surface. Instead of the normal component, two tangential component are matched to the given magnetic field. This modification doubles the number of unknowns to be solved in the resulting linear system of equations, but allows the use of the Fast Multipole Method and eliminates the problem with the Dirac strings and current loops. The Fast Multipole Method can also be used to accelerate the iterative solver, largely compensating for the bigger number of variables.

The relative precision of the reproduction of the magnetic field is typically about 10^{-3} using 10^4 sources for a magnet with length of 1 meter. The precision can be made better by increasing the number of point sources. Regardless of the error relative to the reference field, the reconstructed field is continuous and satisfy Maxwell's equations close to machine precision anywhere inside the volume of interest. This is a key feature of the SIMPA algorithm, and it is the reason of the reconstruction of the field with point sources.

The distance of the point sources from the surface is a free parameter, but it must be chosen carefully. The elevation should be such, that the point sources are not too close to the boundary surface of the element, because the point sources can not be inside the balls of the cover or too close to them. When the sources are too close to the balls, the field expansion will require higher degree spherical harmonics which will make the field map slower and bigger or even impossible to achieve the required level of discontinuity between

TUPAM1R3

STATUS OF BEAM INSTRUMENTATION AT THE ELECTRON BEAM TEST STAND AT CERN

M. Sameed*, M. Ady, S. Burger, J. Cenede, A. Churchman, T. Coiffet,

W. Devauchelle, A. Ganesh, A. Kolehmainen, S. Mazzoni, D. Perini, M. Plantier,

A. Rossi, S. Sadovich, Y. Sahin, G. Schneider,

O. Sedlacek[1], C. Castro Sequeiro, K. Sidorowski, R. Veness, F. Guillot-Vignot, M. Wendt

CERN, Geneva, Switzerland

P. Forck, S. Udrea

GSI, Darmstadt, Germany

O. Stringer, C. Welsch, H. Zhang

The University of Liverpool, Liverpool, UK

[1]also at The University of Liverpool, Liverpool, UK

Abstract

The Electron Beam Test Stand (EBTS), a collaborative effort at CERN with the Accelerator Research and Innovation for European Science and Society (ARIES) project, has been purpose-built within the High Luminosity Large Hadron Collider (HL-LHC) initiative. This comprehensive test facility features a high-perveance electron gun producing a hollow electron beam, supported by a magnetic system comprising normal conducting solenoid magnets with horizontal and vertical correctors. The EBTS boasts an array of advanced beam instrumentation, including YAG:Ce screens, a multi-channel Pin-Hole Faraday cup, a Beam Position Monitor (BPM), and a Beam Gas Curtain (BGC) profile monitor integrated with an optical transition radiation (OTR) screen. Additionally, it includes an electron collector.

This paper offers an overview of the EBTS, emphasizing the design and capabilities of its various beam instruments. It further provides insights into some prototype test results with pulsed electron beams, and upcoming tests with DC beams. The EBTS holds great potential as a valuable tool for advancing electron beam technologies, particularly in the realm of sources and instrumentation for electron cooling devices.

INTRODUCTION

The EBTS at CERN has been designed and constructed to address the objectives outlined in ARIES WP16 (Intense, RF Modulated, E-Beams (IRME)) [1–3], as well as HL-LHC WP5 (Collimation) and WP13 (Beam Instrumentation) [4]. The key objectives include:

- Designing and building a test stand capable of evaluating an electron gun, equipped with instrumentation for measuring both transverse and longitudinal profiles of the RF-modulated electron beam.
- Conducting measurements to characterize the properties of the RF-modulated electron beam generated by the gun within this test stand.

---

* m.sameed@cern.ch

- Prototyping components, such as the electron gun, collector, and BPM, to potentially implement hollow electron lenses (HEL) for active beam-halo control in the HL-LHC.
- Developing a gas curtain monitor to precisely align the electron and proton beams within the hollow electron lens.

Although the ARIES project concluded in 2022, the R&D part of the HL-LHC project remains ongoing. This section will delve into specific aspects of the HEL and their implications on the design of the EBTS. The EBTS will be described in subsequent sections along with an update on the current status of beam instrumentation at this facility.

High Luminosity LHC Hollow Electron Lens

The purpose of HEL is to enhance the transverse beam halo diffusion and provide controlled halo depletion for HL-LHC proton beams [5]. By superimposing a low-energy (about 10 keV), high-current (5 A) counter-propagating hollow electron beam with the proton beam, halo particles in the proton beam experience non-linear transverse kicks, while the particles in the beam core remain unaffected. Over time, these kicks accumulate, diffusing and eventually removing halo particles through downstream collimation. The electron beam must be concentric with the proton beam (within 100 μm) over a three-meter interaction region to achieve 90 % halo depletion in five minutes [6, 7].

The key components for HEL, as depicted in Figure 1, include the electron gun and pulse modulator for generating the pulsed hollow electron beam. Two beam position monitors are employed to precisely locate the proton and electron beams in the interaction region. The minimally invasive beam profile monitor, known as the BGC (for Beam Gas Curtain monitor) [8–14], acts as an overlap monitor for both beams. Additionally, a collector serves as an electron beam dump. The setup also features superconducting solenoids, compensation magnets, and steering coils to guide and control the beams within their designated orbits.

The HEL prototype components to be tested at the EBTS include the electron gun, BPM, BGC, and electron collector.

DEVELOPMENT OF STOCHASTIC COOLING COMPONENTS FOR HIAF SPECTROMETER-RING

G.Y. Zhu[1,†], J.X. Wu[1], Z. Du[1], J. Yin, IMP CAS, Lanzhou, China
L.Y. Ma, Northwest Normal University, Lanzhou, China

Abstract

Stochastic cooling of the spectrometer ring (SRing) with the bandwidth of 0.6-1.2 GHz at the High Intensity Heavy-Ion Accelerator Facility (HIAF) project in China, which is used mainly for experiments with radioactive fragment beams, is applied to speed up the cooling process of a stored ion beam. In this paper, both the prototypes of coaxial notch filter with amplitude equalizer and optical notch filter with phase-stabilized optical fiber cable are built and measured for SRing stochastic cooling system. A 9 bit wide-band 360° digital adjustable phase shifter with minimum step length of 0.7° has been fabricated and tested for HIAF stochastic cooling. Meanwhile, the prototype of RF signal transmission processing units of SRing stochastic cooling are measured. Finally, the development, performance, and testing of both a Faltin prototype traveling wave structure and a novel slot-ring prototype standing wave structure based on a ceramic vacuum chamber for the HIAF SRing stochastic cooling system are discussed briefly.

INTRODUCTION

The High Intensity Heavy-Ion Accelerator Facility (HIAF) project was proposed by the Institute of Modern Physics (IMP) of the Chinese Academy of Sciences (CAS) in 2009. It will provide high intensity heavy-ion beams for nuclear physics, atomic physics, and other applications [1]. As an essential part of HIAF, the high-precision spectrometer ring (SRing) is designed to perform nuclear mass spectrometry in combination with fast beam cooling [2]. Stochastic cooling of the SRing, which is used mainly for experiments with radioactive fragment beams, plays a significant role in beam cooling and is applied to speed up the cooling process of the stored ion beam. The stochastic cooling system of SRing mainly consists of pick-ups, kickers, RF power amplifiers, and signal processing and transmission equipment, which are designed to operate with the operating bandwidth of 0.6-1.2 GHz [3]. Figure 1 shows the layout of the SRing stochastic cooling system. Notch filter, broadband phase shifter and pickup/kicker are one of the most critical devices for SRing stochastic cooling system.

† email address: zhuguangyu@impcas.ac.cn
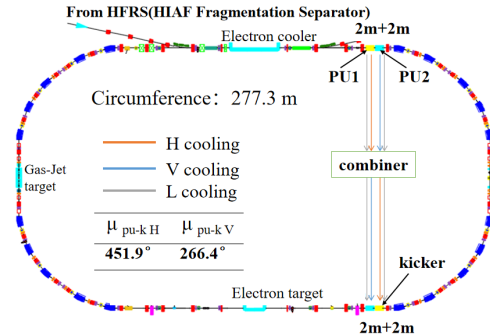
Figure 1: Layout of the stochastic cooling system on the SRing.

NOTCH FILTER

The ideal notch filter consists of a in-phase splitter, a short and a long transmission line, and a 180° microwave hybrid. The schematic drawing of an ideal notch filter is shown in Fig. 2.
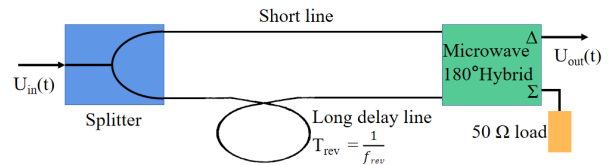
Figure 2: Schematic drawing of an ideal notch filter consisting of a splitter, a short and a long transmission line, and a "subtractor" (a microwave hybrid with a 180° phase-shift in one branch).

In order to improve the notch depth of the notch filter, both the coaxial notch filter with an amplitude equalizer in the long branch and the optical notch filter with a phase-stabilized optical fiber cable are developed, performed, and measured for the SRing stochastic cooling system [4]. The coaxial notch filter with amplitude equalizer in long branch mainly consists of a power splitter, a short coaxial cable and a long coaxial cable transmission line, electrical programmable delay line, amplitude equalizer, variable attenuator, 50 Ω load and 180° microwave Hybrid, as shown in Fig. 3(a). The optical notch filter with a phase-stabilized optical fiber cable consists of RF/optical transmitter and optical/RF receiver, optical power splitter, short and long phase-stabilized optical fiber, variable optical electrical delay, variable optical attenuator, 50 Ω load and 180° microwave hybrid, as shown in Fig. 3(b). The notch depth of coaxial notch filter is also measured by VNA from 600 to 1200 MHz, the minimum and maximum notch depth are approximately 26 dB at 650 MHz and 57 dB at 800 MHz respectively. The notch depth of optical notch filter is also

NUMERICAL STUDY OF THE WIGGLER-BASED MICROBUNCHING AMPLIFIER FOR EIC*

C. Hall, RadiaSoft LLC, CO, Boulder, USA

A. Zholents†, Argonne National Laboratory, Argonne, IL, USA

Abstract

An amplifier of microbunching instability in the electron beam employing wiggler magnets is considered. A lattice design is described. The impact of the SASE FEL resonance is analysed. A setup for macro particle tracking and a method for microbunching gain determination is presented. Calculations demonstrate feasibility of a broad band amplifier with a large gain.

INTRODUCTION

Coherent electron cooling [1] using a plasma-cascade amplifier (PCA) [2] can provide significantly faster cooling of hadrons than the conventional method of microwave stochastic cooling due to the wide bandwidth of a pickup, a kicker, and an amplifier. The PCA creates unstable plasma oscillations by varying the transverse beam size along the beam line, thus modulating the plasma frequency. An alternative approach to the amplifier is to modulate the plasma frequency by a sequence of wiggler magnets separated by weak chicanes [3]. Numerical simulations of the gain function are done using OPAL-FEL code [4] and the electron beam parameters projected for the Electron Ion Collider.

LATTICE OF THE AMPLIFIER UNIT

The basic cell of the Wiggler Enhanced Plasma Amplifier (WEPA) is composed of a wiggler and quadrupole triplet, with the triplet providing transverse matching into subsequent cells. Parameters of the wigglers used in all simulations presented here are given in Table 1.

Table 1: Wiggler Parameters

Parameter	Value	Unit
Wiggler length ℓ_W	1.188	m
Wiggler period λ_W	3.3	cm
Wiggler parameter K_w	1.5	
Wiggler peak magnetic field B_{peak}	0.487	T
Bending radius ρ	1.076	m
Wiggler magnetic gap	16.0	mm

Chicanes are placed to convert the accumulated energy modulation into additional density modulation after a set of cells. Two identical chicanes are used for convenience. We refer to a set of several wiggler and triplet cells, followed by chicanes as a single amplifier *unit*. The total length occupied by the chicanes is equal to the wiggler length such as to
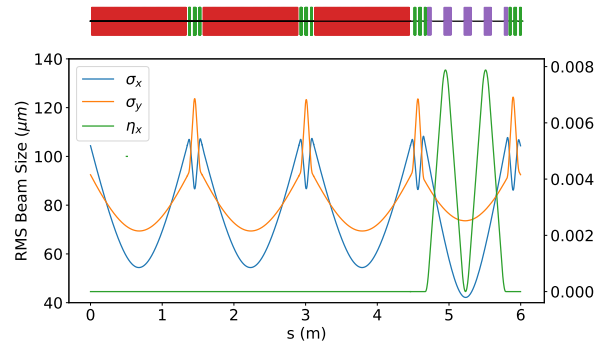
Figure 1: Lattice of a single amplifier unit with three cells followed by two chicanes. Transverse RMS beam sizes and dispersion function are shown. Locations of wigglers, triplets, and chicanes are shown at the top.

minimize a perturbation to the lattice. The basic chicane parameters are given in Table 2.

Table 2: Chicane Parameters

Parameter	Value	Unit
R_{56}	0.5×10^{-3}	m
Dipole length l_b	0.05	m
Dipole bend angle θ_b	1.96	degrees
Dipole field	0.04	T
Chicane leg L	0.18	m

Accounting for the wiggler focusing and transverse space charge effects necessitated slight modifications to the matched Twiss functions and focusing strengths of the quadrupoles comparing to a lattice in which drifts are used instead of the wigglers. To ensure that a wiggler and triplet cell is matched a numerical optimization of the initial transverse conditions of the bunch and the quadrupole strengths in the triplet was carried out with particle tracking through one cell in OPAL-FEL.

The main concerns related to use of the chicanes in the lattice are the nonlinear compression terms and coherent synchrotron radiation (CSR). Because of a small R_{56}, the weak dipoles are used and the overall impact of non-linearity and CSR is small. Indeed, the growth in energy spread in the chicane after the second amplifier unit for a bunch with peak current of 165 A and with an initial modulation wavelength of 2.88 μm, where the gain in the second unit is close to 80, is around 7 %. The simulations for the chicane were carried out using the particle tracking code `elegant` [5]. The resulting matched beam with lattice overlaid is shown for a three-cell unit in Fig. 1. For simulations involving more

SELF BUNCHING, RF BUNCHING AND COOLING OF IONS IN AN ELECTROSTATIC ION BEAM TRAP

D. Sharma[1, *], D. Zajfman[1], O. Heber[1], R. Ringle[2]
[1]Department of Particle Physics and Astrophysics, Weizmann Institute of Science, Rehovot, Israel
[2]Department of Physics and Astronomy, Michigan State University, East Lansing, Michigan, USA

Abstract

We describe the beam dynamics in an electrostatic ion beam trap (EIBT). The ion-ion interaction plays a crucial role in governing the beam dynamics in the trap. We show that the EIBT can serve as a unique device for phase space manipulation of the ions. Three important results are presented: 1. Self-bunching of ions where the ion-ion interaction which is a repulsive Coulombic interaction provides the necessary coupling to keep the ions synchronized, 2. RF bunching of ions, where the repulsive ion-ion interaction keeps the ion bunch localized in the RF bucket and suppresses the emittance growth, 3. Auto-resonance cooling of ions, where a slice from phase space is accelerated out and cooled by evaporation.

ELECTROSTATIC ION BEAM TRAP

Electrostatic ion beam trap is a unique and versatile device to store ion beam with no mass limit [1]. A schematic is shown in Fig. 1. The ions are trapped between two sets of mirror electrodes. The motion of ions is detected by the pickup electrode placed at the center of the trap. The inner electrodes for the two mirrors are at the ground which provides a filed free region in the trap. The ions dynamics in the trap are governed by the slip factor η,

$$\eta = -\frac{2E}{f}\frac{df}{dE},$$

where f represents the oscillation frequency of the ion trapped in EIBT with energy E. The trap can be operated in dispersive or self-bunching regime by changing the sign of the slip factor which is decided by the potential profile in the trap. An external time-dependent voltage can be applied to V_5 of the mirror electrode (see in Fig. 1). A bunch of positively charged SF_5^+ ions produced by the Even-Lavie ion source is accelerated to 4.2 keV, focused, and steered using the Einzel lens and XY deflector before being injected into the trap. The density of ions in the trapped can be monitored by adjusting the voltage on the entrance electrode V_P. The time signal obtained from the pick-up electrode is collected by a digitizer and analysed using Fourier transform to obtain the frequency distribution of the ions bunch. This trap is unique and different from the other storage rings or trap devices, since the ion density oscillates in the trap. A typical number of ions in a bunch in the field-free region is $10^5 - 10^7$. The ion density in the turning point can be ~10^3 orders higher than the field-free region. The ion-ion interaction (collisions) is important at the turning point and affects the beam dynamics in the trap. The ion-ion interaction also couples the transverse and longitudinal beam dynamics in the trap. The dynamics of ions in the trap can be simulated with a simulation technique based on particle-in-cell (2DCYLPIC). The simulation can consider the space charge effect and all the experimental results are well reproduced [2].

DISPERSION AND SELF BUNCHING

When a bunch of ions are injected in the EIBT, depending on the potential profile either it will disperse or stay localized in the trap. The dispersion and synchronization of ions in EIBT are studied very well with detail [3, 4]. A
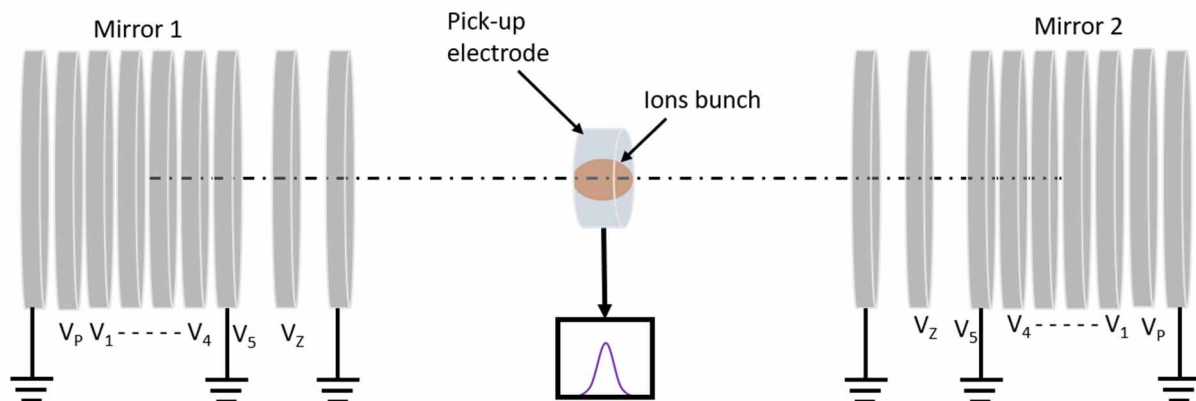
Figure 1: A schematic of electrostatic io beam trap. The ions are trapped between two sets of mirror electrodes and the passage of ions bunch is monitored by pick-up electrode.

* deepaks4894@gmail.com

THEORETICAL AND SIMULATION STUDY
OF DISPERSIVE ELECTRON COOLING *

H. Zhao[†],L.J Mao, M.T. Tang, F. Ma, X.D. Yang, J.C. Yang
Institute of Modern Physics, Chinese Academy of Sciences, Lanzhou, China

Abstract

In electron cooling, the transverse cooling rate is usually smaller than the longitudinal rate, especially at high energies. By introducing dispersive cooling, it is possible to redistribute the cooling rate between longitudinal and transverse planes. Theoretically, achieving dispersive electron cooling requires an ion dispersion and a transverse gradient of longitudinal cooling force. The latter depends on many factors such as beam energy offset, transverse displacement, e-beam density distribution and space charge effect. Therefore, several methods can be employed to achieve dispersive electron cooling based on these factors. In this paper, these factors and their respective impacts on the cooling rate are discussed. Based on a linear friction force model, we propose a simple formula to numerically estimate the cooling rate redistribution effect of these methods. The analytical results are in good agreement with Monte-Carlo calculation and numerical simulation.

INTRODUCTION

In theory, dispersive cooling requires both ion beam dispersion and a transverse gradient of the longitudinal cooling force [1]. To simply explain that, we assume an off-momentum particle passing through the cooling section with a dispersion function D, and only consider the longitudinal cooling with a linear cooling force $\Delta\delta_p = -\lambda\delta_p$, the particle coordinate after cooling can be written by

$$x_{\beta2} = x - D\delta_{p2} = x_{\beta1} + D\lambda\delta_{p1}, \quad (1)$$

where x_β denotes the betatron oscillation, and x is the real coordinate which is assumed to be unchanged during passing through the cooling section. If the cooling coefficient λ is a constant, the amplitude of the betatron oscillation keeps unchanged $x_{\beta2} = x_{\beta1}$, which means that there is no cooling contribution from the longitudinal direction to the transverse. Otherwise, if the cooling force has a transverse gradient, for example $\lambda(x) = (M - |x|)\lambda_0$ with $M > Max[x]$, the amplitude of the oscillation turns to $x_{\beta2} \simeq (1 - \lambda_0|D\delta_{p1}|)x_{\beta1}$. It indicates amplitude damping of the betatron motion. A schematic plot of these two processes is shown in Fig. 1, where the x-axis represents betatron oscillation under longitudinal cooling of the y-axis. It clearly shows the amplitude damping process with an appropriate longitudinal cooling force setting, i.e. dispersive cooling.

We see that the transverse gradient of the longitudinal cooling force plays a key role in dispersive electron cool-
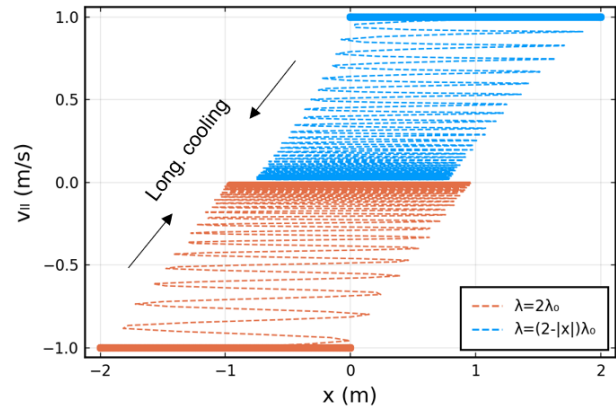
Figure 1: Comparison of the cooling process with two sets of longitudinal cooling force. It demonstrates that a dispersion and a transverse gradient of the longitudinal cooling force are necessary for dispersive cooling ($x_\beta = 1\,\mathrm{m}$, $D = 1\,\mathrm{m}$, $\delta_p = \pm1$, $\lambda_0 = 0.01$).

ing. Some experimental and simulation studies have demonstrated several approaches to obtain this gradient. As indicated in Ref. [2, 3], one approach is to introduce a displacement between electron and ion beams, utilizing the parabolic velocity profile of the electrons caused by its space charge. Another method is by using an energy offset, a displacement and a transverse density gradient of the e-beam [4]. Recently, it has been demonstrated that an e-beam with Gaussian transverse distribution can naturally provide this transverse gradient, thus achieving dispersive cooling [5]. At the same time, it shows that electron dispersion is also beneficial to dispersive cooling. In this article, we conduct theoretical and simulation studies of these methods and show how they affect the cooling rate. Based on the linear cooling force model, we finally propose a simple formula to numerically estimate the cooling rate redistribution effect of these methods, and the analytical result agrees well with Monte-Carlo calculation and numerical simulation.

DISPERSIVE ELECTRON COOLING

To begin with, we assume a linear cooling force $\Delta u = -Cn_eu$ both in transverse and longitudinal directions, where n_e is the electron beam density, C is the cooling coefficient which depends on the velocity distribution of the electron beam. Consider a beam displacement x_o, an energy offset δ_o, and horizontal dispersion D of ions in the cooling section, the momentum change of a single particle after cooling can be described by $\Delta\delta \simeq -C_pn_e(\delta - \delta_e - \delta_o)$, where $\delta_e = K_{sc}(x^2 + y_\beta^2)$ is the electron momentum deviation due

---

SUSTAINING COMPETENCES FOR ELECTRON COOLING AT HESR

Kurt Aulenbacher, Thomas Beiser, Juergen Dietrich, Wolfgang Klag
Helmholtz Institute Mainz (HIM), Germany

Abstract

The HESR storage ring will be operated with a high intensity antiproton beam to serve the PANDA experiment.

Due to several reasons its completion is presently postponed which causes the issue how to keep competences required to develop and operate the electron cooler. We will present mitigation plans that will enable Helmholtz-Institut Mainz (HIM) to pursue its goals even if the present situation would last for a long time.

INTRODUCTION

The research group ACID-II at Helmholtz Institute Mainz (HIM) is aiming to resolve technical challenges related to high energy electron cooling. This is connected to a possible relativistic magnetized electron cooler for the High Energy Storage Ring HESR at FAIR. An electron kinetic energy of almost 8 MeV would be required, exceeding the voltage of the Jülich cooler [1] considerably, which is currently the cooler with the highest voltage and magnetized beam.

In cooperation with the Budker Institute for Nuclear Physics (BINP) at Novosibirsk in Russia we have proposed a modular concept based on high voltage platforms, each delivering a potential of 600 kV. The floating electric power is provided by turbogenerators which supply the solenoids and auxiliary devices such as electron source, collector-supply, or vacuum pumps. A first module was built by BINP and delivered to Mainz [2]. These modules – called platforms - are intended to be 1:1 scale size prototype for the HESR-cooler.

Since the last conference of this series all HESR related projects have been confronted with uncertainties because of cost increases and the political situation. These will probably lead to an additional delay of several years before HESR can start operation. In particular, the cooperation with most Russian institutions has been suspended and it is presently not clear when such co-operations will become possible again. This also applies to our plans to test the scalability with more than one HV-platform.

In this paper we describe the progress we have achieved since the last conference COOL'21 and try to sketch a strategy how to sustain the competences that have been gained at HIM until the timeline of the HESR becomes more predictable.

PLATFORM OPERATION

The arrangement was described in the paper covering our status at COOL'21 [2] where more details can be found. A pressure tank of 4 m inner diameter is intended to hold a stack of 600 kV high voltage platforms (Fig. 1).

---

† aulenbac@uni-mainz.de

Since the cooperation with BINP was suspended, no delivery of the second platform took place. This will inhibit our tests for scalability until either the cooperation is resumed, or we build the other stages from our own means. The latter is feasible but would require considerable engineering capacity. Considering the delays in the timeline of HESR it seems reasonable to postpone such decisions and restrict ourselves to operation of the first 600 kV platform. We will operate the gas-expansion turbines for power generation with dry nitrogen at the beginning. An input pressure of 3 bar can be generated by our screw compressor with a mass-throughput that suffices to drive at least two turbines. It was considered most favourable to use a closed Nitrogen circuit, i.e., feeding the exhaust gas of the turbines back to the compressor, the input and the exhaust flanges can be seen in Fig. 2. In first tests it turned out that stable operation of the system, e.g., when changing the load on the turbine, was difficult to achieve.
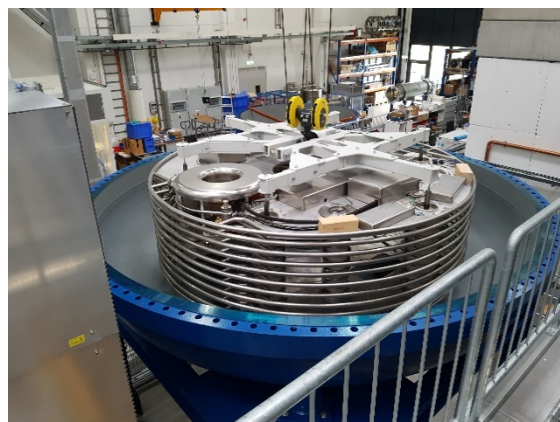
Figure 1: Lower part of HV tank at HIM with first platform installed. Inner diameter of tank is 4 meters.

In cooperation with Prof. Wirsum from the Institute for turbo electric power generation at RWTH Aachen a thorough analysis of the pneumatic circuit was completed [3]. The reasons for the instabilities were identified and countermeasures proposed. The modifications were delayed by the supply chain problems that occurred during 2022, for instance by a very long delivery time for regulation valves. However, the modifications were finalized in spring 2023 and stable operation of a turbine in the closed cycle configuration was achieved. As a next step we will connect the already installed turbine on the 600 kV platform to the circuit. In this configuration the gas supply line is made from insulating material and integrated into the platform. Later, HV-tests will start, with the goal to reach 600 kV operation. This step will be challenging because the support from the designers of the platform at BINP is presently missing. To have stable HV-conditions on the platform, the supply lines and the turbine will be exposed to a moderate overpressure

THPAM1R2

STATUS OF E-COOLING CHARACTERISATION AT 100 keV IN ELENA

D. Gamba*, F. Asvesta, P. Kruyt[1], L. Ponce, and G. Russo

CERN, 1211 Geneva, Switzerland

[1] also at Goethe University, Frankfurt, Germany

Abstract

The Extra Low ENergy Antiproton ring (ELENA) ring at CERN was commissioned in 2018 and has been in regular production operation since 2021. ELENA uses e-cooling for cooling antiproton (pbar) beams on two plateaus at 653 keV and 100 keV kinetic energy. The first cooling is necessary to allow for efficient deceleration of the 5.3 MeV pbar beam coming from the Antiproton Decelerator (AD), while the second cooling is used to define the quality of the bunches before extraction. The experience accumulated so far shows that cooling at 653 keV is sufficient to ensure good deceleration efficiency, while cooling at 100 keV might not be enough to provide the design transverse beam emittances at extraction. In this paper, we document the present ELENA e-cooling performance at 100 keV, the typical optimisation procedure used during setup, and we investigate possible limitations of the present system.

INTRODUCTION

The ELENA ring is part of the Antimatter Factory at CERN, which is a unique facility that provides pbar beams for low energy antimatter physics [1, 2]. Pbars are produced in the AD target area by sending a 26.4 GeV/c proton beam on an iridium-based target. The emerging pbars at 3.575 GeV/c are guided and collected into the AD ring which cools and decelerates them down to 5.3 MeV kinetic energy. They are then transferred to the ELENA ring which further decelerates and cools them down to 100 keV kinetic energy. Here, four bunches are produced and distributed to up to four experiments at the same time. An overall parameter to assess the antimatter factory performance is the number of pbars delivered to the users as a function of protons sent on target. This is shown in Fig. 1, in which about four weeks of data from 2022 is compared to an equivalent period in 2023. Continuous optimisation of the AD target area and transport allows to regularly reach a pbar yield of 3×10^{-6} pbar injected in AD per proton delivered on target. Proton intensity from the CERN injectors was increased during 2022 and 2023 runs in steps from about 1.4×10^{13} to about 1.7×10^{13}. This, together with improved deceleration efficiency, allowed to increase the number of pbars to more than 5×10^7 injected in AD and more than 4×10^7 in ELENA. Each user requesting beam is now typically receiving 9×10^6 pbar, which is about a factor of 2 higher than the design value.

In the following sections, an update on the ELENA cycle and its hardware will be outlined followed by the latest measurements of e-cooling characterisation with emphasis on the extraction plateau at 100 keV.

---

* davide.gamba@cern.ch
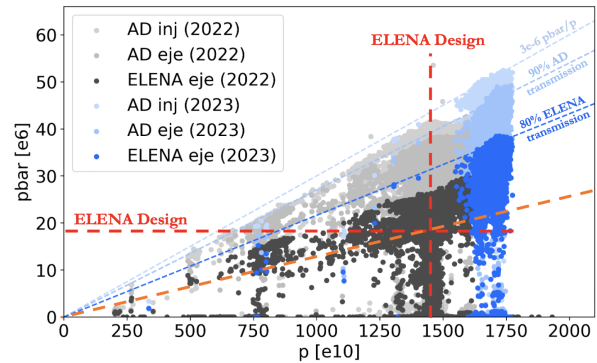
Figure 1: Antiproton intensity as a function of protons on AD target. Pbars measured at AD injection, ELENA injection and ELENA extraction are indicated from lighter to darker colors. Shades of black and blue indicate 2022 and 2023 data, respectively. Proton on target and ELENA extraction design parameters are also indicated in dashed red.

ELENA CYCLE AND INSTRUMENTATION

The ELENA magnetic cycle and available instrumentation are basically unchanged with respect to what is reported in [3]. On top of the regular operation with pbar, ELENA can still be operated with H^- from its local source [4, 5], which continues to be an essential asset for machine setup.

The typical magnetic cycle, basically identical for both pbar and H^- operation, is shown in Fig. 2. During H^- operation the beam is injected at the lowest plateau at 100 keV, it is accelerated to pbar injection energy (5.3 MeV), and then it follows the nominal deceleration cycle as for the pbar. The lifetime of H^- beam is of the order of 5 s, mainly driven by the average ring pressure level which settled at about 1×10^{-11} mbar, while no sizable lifetime degradation via interaction with the electron beam of the e-cooler has been observed so far.

Due to the sizeable H^- beam intensity reduction after deceleration, a second injection at the beginning of the last e-cooling plateau is performed, so to obtain H^- beams at extraction of comparable intensities to the pbar ones.

The ELENA e-cooler [6] was commissioned in 2018 [7], and so far did not require any modifications nor major maintenance. Its main parameters are summarised in Table 1. Since e-cooler parameters cannot be quickly changed between H^- and pbar cycles operation, and hence the electron velocity is fixed, the H^- momentum at the different plateaus is adjusted to match the pbar revolution frequency.

The main instrumentation for e-cooling setup and adjustment remains the Schottky signal, which in ELENA is obtained by combining the signal of several Beam Position

INFLUENCES OF THE LONGITUDINAL SHIFT OF THE ELECTRON BUNCH TO THE LONGITUDINAL COOLING RATE*

G. Wang†, A. Fedotov, D. Kayran

Collider-Accelerator Department, Brookhaven National Laboratory, Upton, NY, USA

Abstract

As two major techniques of cooling a bunched hadron beam in a storage ring, both coherent electron cooling and rf-based traditional electron cooling involve overlapping the cooling electron bunches with the circulating ion bunch. A longitudinal offset of a cooling electron bunch with respect to the ion bunch centre is often introduced, either to cool a single ion bunch with multiple electron bunches or to cool the ions with large synchrotron amplitude more efficiently, i.e. painting. In this work, we derive how the cooling rate is affected by such a longitudinal offset. We use the EIC pre-cooler as an example to study how different overlapping pattern of the cooling electron bunches, e.g. the number of the cooling electron bunches and their longitudinal positions, affect the evolution of the circulating hadron bunches.

INTRODUCTION

Cooling hadrons with a bunched electron beam often involves overlapping one hadron bunch with multiple electron bunches so that the cooling rate can be increased. Examples for such cooling systems include the Low Energy RHIC electron Cooling (LEReC) system [1] and the pre-cooler designed for the Electron Ion Collider (EIC) [2]. Due to the variation of the ions' longitudinal density and their synchrotron oscillations, electrons sitting at different location along the ion bunch have different contributions to the cooling process. It is important to evaluate how the cooling performance changes with the locations of cooling electron bunches with respect to the hadron bunch so that they can be optimized to achieve more efficient cooling. Another example for cooling the hadron bunch with the longitudinally shifted electron bunches is cooling with painting. Since the cooling rate is usually more efficient for hadrons with small synchrotron oscillation amplitudes, the longitudinal profile of the hadron bunch can deviate from Gaussian and a dense core may form after being cooled for some time, which may lead to single bunch instability and degradation of beam lifetime due to large space charge tune shift. One way to counteract the non-uniformity of the cooling rate is to modulate slowly the longitudinal locations of the electron bunches, i.e. painting. Evaluating the cooling rate in the presence of painting also requires calculation of how the cooling rate depends on the longitudinal offset of the electron bunch.

In this work, we derived an analytical formula to calculate the cooling rate as a function of the ion's synchrotron oscillation amplitude with the cooling electron bunch longitudinally shifted away from the ion bunch centre.

AVERAGING THE COOLING RATE OVER SYNCHTROTRON OSCILLATION

We consider a hadron circulating in a storage ring. Due to the energy kick in the RF cavities, the ion carries out synchrotron oscillation as shown in Fig. 1.
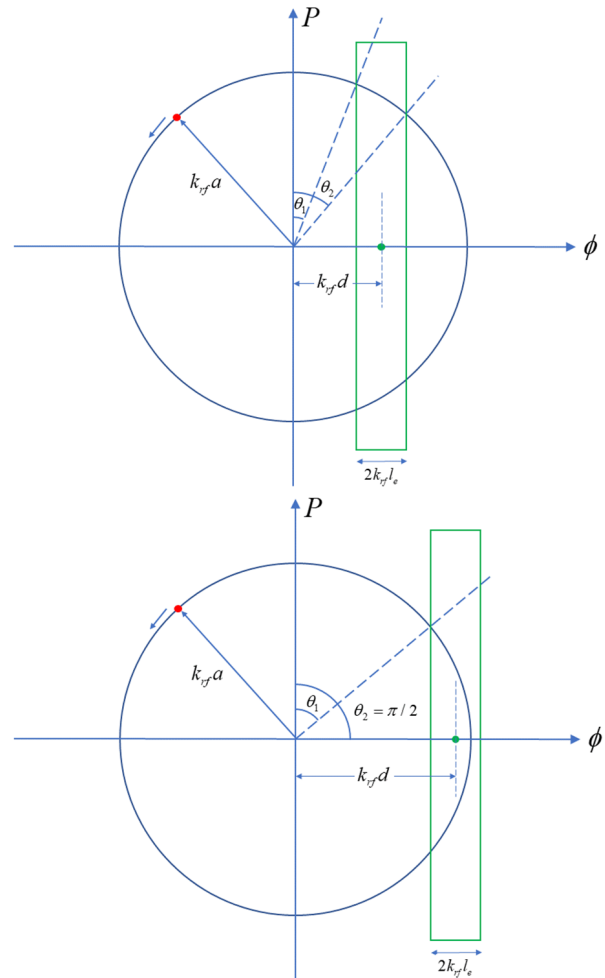
Figure 1: Illustration of the longitudinal cooling of an ion with synchrotron oscillation amplitude ϕrf_{max} and a cooling electron bunch with bunch length of $2l_e$ and offset of d. The red dot represents the ion and the green box represents the region in the ion's longitudinal phase space covered by the cooling electron bunch, i.e. the ion is overlapping with the electrons when it gets into the box. The green dot represents the centre of the electron bunch. The abscissa is the RF phase of the ion and the ordinate is the normalized energy deviation.

Figure 1 shows two cases of the ion conducting synchrotron oscillation in its phase space with the abscissa and

ADVANCEMENTS AND APPLICATIONS OF COOLING SIMULATION TOOLS: A FOCUS ON Xsuite

P. Kruyt[*][1], D. Gamba, G. Franchetti[1,2,3]
CERN, Geneva, Switzerland
[1]also at Goethe University, Frankfurt, Germany
[2]also at GSI, Darmstadt, Germany
[3]also at HFHF, Frankfurt am Main, Germany

Abstract

This paper presents recent advancements in cooling simulation tools in Xsuite, which is a new particle accelerator simulation code developed at CERN. An electron cooling module, based on the Parkhomchuk model, has been implemented and benchmarked against Betacool using parameters of the LEIR e-cooler at CERN. Additionally, a laser cooling module has been implemented, capable of simulating various laser pulse types, including Fourier-limited and continuous wave lasers. This module is applied to the Super Proton Synchrotron (SPS) with the aim of simulating the Gamma Factory proof-of-principle experiment (PoP) at CERN. First results are presented.

INTRODUCTION

The goal of this paper is to present the electron cooling and the laser cooling module of Xsuite and their respective advantages compared to other tracking codes. Xsuite is a collection of Python packages for multi-particle simulations for particle accelerators. It has been under development at CERN since 2021 and it has the capability to run on both CPUs and GPUs [1]. As for electron cooling, two currently available codes that also incorporate the Parkhomchuk model of electron cooling [2, 3] are Betacool [4, 5] and JSPEC (JLab Simulation Package for Electron Cooling) [6, 7]. The main advantage that Xsuite provides over Betacool is that it is under active development, whereas Betacool is no longer active. In comparison to JSPEC, Xsuite offers GPU capability and offers a wide variety of features beyond electron cooling, including synchrotron radiation, beam-beam effects, electron cloud, etc.

As for laser cooling, the Xsuite module is the first publicly available code that simulates laser cooling in particle accelerators with a great level of detail. While Betacool does offer laser cooling capabilities, it does not have an elaborate excitation scheme like Xsuite. The main goal of the new Xsuite module is to provide tools for simulating the beam cooling in the Gamma Factory [8–12], which is part of the Physics Beyond Colliders (PBC) study at CERN that aims to generate intense beams of scattered photons. Before the implementation of the Gamma Factory in the Large Hadron Collider (LHC), a proof-of-principle (PoP) experiment is intended to be carried out in the Super Proton Synchrotron

_____
* pieter.martin.kruyt@cern.ch

(SPS). The laser cooling module of Xsuite will be a key tool in simulating these two cases.

ELECTRON COOLING

This work is an expansion of the electron cooling simulation tools developed by N. Biancacci and A. Latina, which were initially used for simulating the impact of IBS on low-intensity cooled beams in LEIR [13, 14]. The electron cooling module of Xsuite has been benchmarked with BETACOOL for the CERN accelerator LEIR (Low Energy Ion Ring) [15]. The benchmark compares the implementation of the Parkhomchuk model in both codes. The first part of the benchmark is done by comparing the time evolution of the emittance. The second part compares the cooling force as a function of the velocity difference between the circulating beam particles and the electrons. The electron cooler parameters are displayed in Table 1. The blue curve in Fig. 1, labeled as SC=0, represents the emittance comparison for a lead coasting beam in LEIR at 18 GeV/c. Here, SC=0 indicates that the space charge effect of the electron beam is inactive. The cooling force comparison is displayed in Fig. 2. The benchmark shows that Xsuite and Betacool produce compatible results for the time evolution of the emittance as well as for the cooling force as a function of the velocity difference. Additionally, the same benchmark was successfully performed for coasting beams in ELENA at 35 MeV/c [16], utilizing the electron cooler parameters provided in [17, 18]. Lastly, the module proved valuable in clarifying the magnetic field straightness requirements for the new AD electron cooler [19].

Table 1: LEIR Electron Cooling Simulation Parameters [20]

Parameter	Value
Electron beam radius	25 mm
Cooler length	3 m
Magnetic field strength	0.07 T
Transverse temperature	10 meV
Longitudinal temperature	1 meV
Current	0.6 A
β_x/β_y in the cooler	5/5 m

Initially, the benchmark between Xsuite and Betacool failed when the electron beam space charge was included. The Xsuite module incorporates two components of the electron beam space charge. Firstly, it incorporates an energy

THPOSRP02

INFLUENCES OF BEAM PARAMETERS ON THE INTERACTION BETWEEN ION AND ELECTRON BEAMS

V. A. Britten*, O. Meusel, H. Podlech[1], A. Schempp

Institute of Applied Physics (IAP), Goethe-University, Frankfurt am Main, Germany

[1] also at Helmholtz Research Academy Hesse for FAIR (HFHF), Frankfurt, Germany

Abstract

Electrons can be confined as a static column or as a comoving beam for applications in accelerator physics. Depending on the configuration of the electrons, they can cool [1], compensate [2] or even focus [3] the ion beam. In the case of an electron beam, the parameters must be chosen correctly to obtain the desired effects. The influences of these beam parameters on the interaction between the ion and electron beam are investigated in numerical simulations by using a particle-in-cell code [4]. The understanding of the different interaction mechanisms will allow an even better matching of the beams to each other for the intended application. With additional suitable beam diagnostics, it will be possible to draw conclusions about the interaction of the superimposed beams in order to evaluate the quality of the settings and, if necessary, to correct them.

SIMULATION SETTINGS
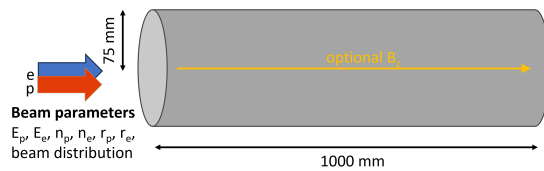
Figure 1: Schematic layout of the simulation setup.

To investigate the influence of the initial beam parameters, simulations were performed by using the particle-in-cell code Bender [4]. A proton beam is superimposed with an electron beam (Fig. 1). The simulation volume is bounded by a beam tube with a radius of 75 mm and a length of 1000 mm. In each simulation, the initial kinetic energies are set to $E_{\text{kin,protons}}$ = 50 keV and $E_{\text{kin,electrons}}$ = 27.23 eV so that the velocities of the beams are the same ($v_e = v_p$). The resulting transit time is τ = 323 ns. The beams start with the same radius ($r_e = r_p$ = 15 mm). In the simulations, in which the mean density is varied to study the influence of the initial density, the initial distribution is chosen the same. In addition, a longitudinal homogenous magnetic field of B = 3 mT is used in some simulations.

Table 1: Initial Beam Parameters

beam particles	E_{kin}	r	distribution
protons	50 keV	15 mm	Gaussian/KV
electrons	27.23 eV	15 mm	KV

* britten@iap.uni-frankfurt.de

DENSITY INFLUENCE

In order to investigate only the influence of a density difference, all other initial beam parameters were left constant in each simulation (see Table 1), while the mean density was varied. A KV distribution was chosen as an initial distribution for the electron and proton beam to ensure linear space charge fields.

Without a Longitudinal Magnetic Field

To allow undisturbed particle interactions, simulations were first performed without a longitudinal magnetic field for different cases. First, the same density for both beams was simulated as a reference. Then, different densities were chosen: $n_e < n_p$ and $n_e > n_p$.

Case $n_e < n_p$:   When the density of the protons is greater than the density of the electrons, the electrons, as they move in the z-direction, begin to oscillate radially around the beam axis, creating focal points of increased density (similar to Fig. 2). This leads to strong non-linear fields, so that a redistribution of both beams can be observed. The kurtosis of the proton beam grows from an initial value of 2 to 2.3 for the case $5n_e = n_p$ and to over 2.4 for the case $1.5n_e = n_p$ (Fig. 3b) while the kurtosis of the electrons (Fig. 3e) increases right at the beginning and oscillates around the value 2.4. This oscillation decreases in the course of the simulation. This redistribution of particles in the beam causes an emittance growth of both beams (Figs. 3a and 3d). Another important effect is the energy shift, which also occurs at different densities. The greater the density difference, the greater the energy shift, which can be seen in Figs. 4 and 5.
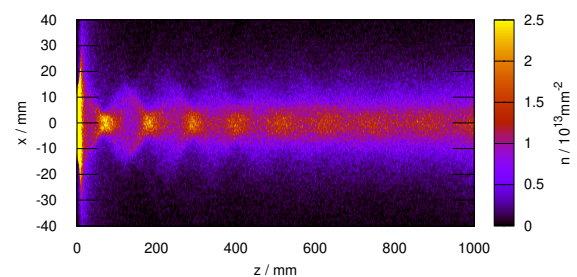
Figure 2: x-z-plane of the electron densitiy distribution for $n_e > n_p$. The electron slice is seen at the beginning, which is a result of the high space charge forces. The following oscillation of the electrons is similar to the oscillation of the electrons in the case $n_e < n_p$.

EXPLICIT EXPRESSIONS FOR NON-MAGNETIZED BUNCHED ELECTRON COOLING*

S. Seletskiy†, A. Fedotov, Brookhaven National Laboratory, Upton, Long Island, NY, USA

Abstract

Recent success of Low Energy RHIC Electron Cooler (LEReC) leads the way in development of high energy electron coolers based on non-magnetized electron bunches accelerated by RF cavities. In this paper we derive explicit formulas for the friction force and the cooling rates in non-magnetized electron coolers in the presence of redistribution of cooling decrements. We further consider several particular cases reducing the general expressions to simple analytic formulas useful for optimization of coolers' parameters.

INTRODUCTION

Redistribution of cooling between longitudinal and transverse directions [1] requires two conditions. The first one is a coupling between the longitudinal and transverse (in this paper we will consider the horizontal one) motion of an ion. This is created by the ions' dispersion in the cooling section (CS). The second condition is dependence of the longitudinal friction force on the horizontal position of an ion in the cooling section, i.e. the longitudinal component of the cooling force must have the transverse gradient. A robust way to create the required gradient (which will be the focus of this paper) is to introduce the electron beam dispersion in the CS.

In the following section we will derive the explicit expressions for the dynamical friction force in the presence of electron dispersion. Next, we will show how introduction of ion dispersion results in $x - z$ redistribution of the cooling rates. Finally, we will apply the obtained formulas to several "asymptotic" cases.

DYNAMICAL FRICTION FORCE

The general expression for the dynamical friction force in non-magnetized cooling is:

$$\vec{F} = -\frac{4\pi N_e e^4 Z_i^2}{m_e} \int \Lambda_C \frac{\vec{v_i} - \vec{v_e}}{|\vec{v_i} - \vec{v_e}|^3} f_e(r_e, v_e) d^3 v_e, \quad (1)$$

where N_e is the number of electrons per bunch, e and m_e are an electron's charge and mass, Z_i is an ion's charge number, v_e and v_i are electron and ion velocities, Λ_C is a Coulomb logarithm, which is a weak function of velocity and can be taken out of integral, and $f_e(r_e, v_e)$ is the electrons 6-D distribution function.

Assuming Gaussian electron distribution, in the presence of electron dispersion (D_e) in the cooling section and using

$x - D_e \delta_e$ for horizontal electron coordinate (here $\delta_e = \frac{v_{ze}}{\beta c}$), one can write f_e in the form $f_e = \rho_e f_{ve}$, where

$$\rho_e = \frac{1}{\gamma (2\pi)^{3/2} \sigma_{1xe} \sigma_{ye} \sigma_{ze}} \exp\left(-\frac{x^2}{2\sigma_{1xe}^2} - \frac{y^2}{2\sigma_{ye}^2} - \frac{z^2}{2\sigma_{ze}^2}\right), \quad (2)$$

$$f_{ve} = \frac{1}{\gamma (2\pi)^{3/2} \sigma_{vxe} \sigma_{vye} \sigma_{1vze}} \times$$
$$\times \exp\left(-\frac{v_{xe}^2}{2\sigma_{vxe}^2} - \frac{v_{ye}^2}{2\sigma_{vye}^2} - \frac{(v_{ze} - \mu)^2}{2\sigma_{1vze}^2}\right), \quad (3)$$

with $\sigma_{1xe} = \sqrt{\sigma_{xe}^2 + D_e^2 \sigma_{\delta e}^2}$, $\sigma_{1vze} = \sigma_{vze} \frac{\sigma_{xe}}{\sqrt{\sigma_{xe}^2 + D_e^2 \sigma_{\delta e}}}$ and $\mu = x \sigma_{vze} \frac{D_e \sigma_{\delta e}}{\sigma_{xe}^2 + D_e^2 \sigma_{\delta e}^2}$.

Now, we can rewrite Eq. (1) as:

$$\vec{F} = -C_0 \rho_e \int \frac{\vec{v_i} - \vec{v_e}}{|\vec{v_i} - \vec{v_e}|^3} f_{ve} d^3 v_e, \quad (4)$$

where $C_0 = \frac{4\pi N_e e^4 Z_i^2}{m_e} \Lambda_C$. We further introduce an effective potential in the velocity-space:

$$U = C_0 \rho_e \int \frac{f_{ve}}{|\vec{v_i} - \vec{v_e}|} d^3 v_e. \quad (5)$$

Noticing that components of the friction force can be presented by $F_{x,y,z} = \partial U / \partial v_{xi,yi,zi}$, one can reduce Eq. (4) to 1-D integrals [2, 3]. For the sake of clarity, we will consider the case of $\sigma_{vxe} = \sigma_{vye} \equiv \sigma_{v\perp e}$ (for detailed derivations and more general cases see [2-4]).

After some algebraic manipulations we get Binney's formulas [5] for friction force components:

$$F_{x,y} = -C_1 \rho_e v_{xi,yi} \int_0^\infty g_\perp(q) dq$$
$$F_z = -C_1 \rho_e (v_{zi} - \mu) \int_0^\infty g_z(q) dq$$
$$g_\perp(q) = \frac{E(q)}{\sigma_{v\perp e}^2 (1+q)^2 \sqrt{\sigma_{v\perp e}^2 q + \sigma_{1vze}^2}} \quad , \quad (6)$$
$$g_z = \frac{E(q)}{(1+q)(\sigma_{v\perp e}^2 q + \sigma_{1vze}^2)^{3/2}}$$
$$E(q) = \exp\left[-\frac{v_{xi}^2 + v_{yi}^2}{2\sigma_{v\perp e}^2 (1+q)} - \frac{(v_{zi} - \mu)^2}{2(\sigma_{v\perp e}^2 q + \sigma_{1vze}^2)}\right]$$

where $C_1 = 2\sqrt{2\pi} N_e r_e^2 m_e c^4 Z_i^2 \Lambda_C$.

To simplify final expressions we will further consider an approximation of small amplitudes ($v_i < \sigma_{ve}$). Then, one can analytically take integrals in Eq. (6). Switching to laboratory frame values $\sigma_{\delta e} = \frac{\sigma_{vze}}{\beta c}$ and $\sigma_{\theta e} = \frac{\sigma_{v\perp e}}{\gamma \beta c}$, we get:

$$F_x = -C_2 \rho_e h v_{xi} \Phi\left(\frac{\sigma_{\delta e}}{\gamma \sigma_{\theta e}} \frac{1}{h}\right)$$
$$F_z = -2C_2 \rho_e h (v_{zi} - K x_i)\left[1 - \Phi\left(\frac{\sigma_{\delta e}}{\gamma \sigma_{\theta e}} \frac{1}{h}\right)\right], \quad (7)$$

where $C_2 = \frac{2\sqrt{2\pi} N_e r_e^2 m_e c Z_i^2 \Lambda_C}{\gamma^2 \beta^3 \sigma_{\theta e}^2 \sigma_{\delta e}}$, $h = \frac{\sqrt{\sigma_{xe}^2 + D_e^2 \sigma_{\delta e}^2}}{\sigma_{xe}}$ and parameter $K = \beta c \frac{D_e \sigma_{\delta e}^2}{\sigma_{xe}^2 + D_e^2 \sigma_{\delta e}^2}$. The function Φ is given by:

A TEST BENCH FOR CHARACTERIZING ELECTRON COOLER COMPONENTS AT UP TO −80 kVDC

G. Khatri*, J. Cenede, A. Frassier, G. Tranquille
CERN, Geneva, Switzerland

Abstract

During the upcoming Long Shutdown 3 (LS3), the electron cooler of CERN's Antiproton Decelerator (AD) will be replaced by a new electron cooler. Present electron cooler is operating at the maximum energy of about 27 keV. However, the new electron cooler will have electron collector and electron gun with the possibility of operating at up to 68 keV electron energy. To characterize the gun and the collector at this higher energy, a test bench has been built and put in operation. The test bench is equipped with a drift solenoid of 1.5 m length operating at 600 Gauss, a Faraday cage with high voltage platform that can be biased up to −80 kVDC. First element of the new AD electron cooler, the electron collector, is presently being tested at the test bench. In this poster we describe in detail the main elements of the test stand, give some highlights of the ongoing tests with the new collector and future plans.

INTRODUCTION

Electron cooling of charged particle beams, originally proposed by G. Budker in 1966 [1], allows to improve quality of the beam by reducing it's emittance. The AD electron cooler was originally built for Initial Cooling Experiment (ICE) at CERN [2] and subsequently modified for use in the Low Energy Antiproton Ring (LEAR) [3] and then in AD [4]. Parts of the cooler are more than 40 years old and lack spares. Therefore decision was made to build a new electron cooler to replace the existing one [5].

Scope of this work is to develop, test and characterize electron gun and collector for the new cooler that can work at least at 2.4 Amp / 27 keV and possibly at higher power. For this purpose a dedicated test bench was put in place. In the section following, a detailed description of the test bench is given. And then some preliminary results of the new collector/gun tests are presented.

TEST BENCH

Figure 1 shows main elements and layout of the test bench. It is a linear test bench, having no bending magnets but only a straight solenoid between the electron gun and the collector. As shown in Fig. 2, the gun is located inside the solenoid at a uniform axial field of 600 Gauss, while the collector is situated at the end of solenoid. At the entrance of the collector a magnetic coil is used to compress the transverse electron beam size, and thus maximising collector efficiency. The high voltage platform consists of a Faraday cage enclosing a 3-phase isolation transformer and two 19"

---

* gunn.khatri@cern.ch

racks on isolation leg posts. The secondary windings of the transformer are floating at the cathode potential provided by an −80 kV power supply that is situated outside the Faraday cage (on ground potential). The high voltage potentials, as illustrated in Fig. 3, are referenced to the cathode by placing the relevant power supplies on the racks inside the Fraday cage. The magnet power supplies are located on the racks at ground potential.

The necessary low vacuum pressure is achieved with the help of turbomolecular pump, titanium-sublimation pump and an ion pump. Due to being more than 20 years old, the achieved vacuum with these pumps is not great. A vacuum bakeout at 150 °C helped remove water and improved overall vacuum and thus electron beam transport. The pressure between the gun and collector in the drift region is estimated to be between 5×10^{-6} and 5×10^{-7} mbar.

The test bench is equipped with safety interlock system that prevents damage to the equipment and allows safe operation for the users. A LabVIEW and python based hybrid control system allows remote control and monitoring of all the power supplies as well as vacuum pressure readout and have logical dependencies on the safety interlock system.

TESTS OF THE NEW COLLECTOR

The original design of the collector underwent a few iterative refinements to mitigate issues related high voltage sparks (e.g. triple junction) in the vacuum before it was able to hold the 30 kV DC bias. However several challenging issues came up before further tests could be done and are described below. Note that the new collector was tested using existing electron gun from AD that operated at nominal beam of 2.4 A and 27 keV.

Observation of Magnetron Discharge

When the magnetic field of 600 Gauss was switched on along with the high voltage, regular and reproducible spikes in the vacuum pressure readout were seen, see Fig. 4. These were understood as magnetron discharges. A surface at relatively negative electric potential would emit an electron which, under crossed electric and magnetic field, would then take a helical path as it accelerates. By collision with the residual gas in the vacuum, it creates secondary electrons and eventually an avalanche. This process repeats when the residual gas replenish in the location of discharge. As this happens, the vcauum is conditioned (by high voltage) and thus the time interval between two consecutive vacuum spikes increases. The solution for getting rid of these discharges was to do a vacuum chamber bakeout. Due to risk of breaking ceramic insulators in the gun and collector, the

AN OPTIMIZED DELAY LINE WITH TEMPERATURE COMPENSATION

N. Shurkhno† and A. Kononov, GSI, Darmstadt, Germany

R. Stassen, FZ Jülich, Jülich, Germany

Abstract

This paper describes the design and development of a low-loss, low-latency optical delay line that provides temperature stability within a given temperature range. Such delays are of particular interest for stochastic cooling systems, where they are used to synchronize a system's correction pulse and in a feedforward loop of optical comb filters. However, commercially available optical delay lines have certain disadvantages for stochastic cooling - large intrinsic delay, high and non-constant optical attenuation, and overall delay drift due to temperature-dependent optical fibers. To mitigate these problems, an optimized optical delay line has been developed for the stochastic cooling systems of COSY (FZ Jülich, Germany) and HESR (FAIR, Germany) accelerator facilities.

INTRODUCTION

There are two main types of variable optical delays – continuous free space delay and stepped optical fiber delay. In free space delays, light travels along a path, whose length can be changed by moving the collimating or reflecting lens with a motor. The motor can continuously change the path length with typical precision of about 1 fs, but the total length is limited to up to a few ns due to the defocusing of the light in free space. In addition, the attenuation varies significantly along the path. To achieve larger delay ranges, step optical fiber delays are used. They are based on routing the light through optical fibers of different lengths in series, called bits (e.g., 0.5 ns, 1 ns, 2 ns, etc.), and provide delay ranges up to ms. The use of optical fiber has certain limitations for such delays. It is temperature dependent, so the intrinsic delay can change dramatically for longer lines, cutting and splicing precision is typically limited to 1 mm, resulting in average accuracy of ~5 ps per bit, and switches, as well as the optical fiber itself, provide different attenuations for different paths, so for multiple bits the total attenuation can vary significantly.

To obtain a long-range optical delay with continuous delay change, the described delays can be combined. Such long-range delays are used, for example, in stochastic cooling systems for signal synchronization and as a delay in an optical comb filters [1, 2]. Such applications have special requirements:

- Low latency, signal propagation in stochastic cooling should be as fast as possible, so the optical delay should provide the lowest possible intrinsic delay.
- Low loss, in stochastic cooling a broadband RF signal is converted to optical and then back to RF, so it is preferable to minimize the optical insertion loss of the delay to eliminate optical or additional RF power amplifiers.

- 1 ps worst-case accuracy and minimal delay fluctuations due to temperature, as systems typically operate continuously for long periods of time.
- Constant attenuation over the entire delay range, which is especially important for an optical comb filter, where even small changes can result in a significantly worse average notch depth.

The requirements are quite specific and challenging, so a simple off-the-shelf solution is not possible, at worst it would require a lot of additional work and testing. To meet all the requirements, a new Optical Programmable Delay Module (OPDM) has been developed (Fig. 1) that provides reduced insertion delay and loss, and continuous delay change over a 128 ns delay range with low attenuation and delay variation and compensated temperature dependence.

Figure 1: Optical programmable delay module (OPDM).

OPTICAL DELAY LAYOUT

The OPDM consists of a precise opto-mechanical free space delay line with a delay range of 0-700 ps and a resolution of 1 fs and an optical step delay with a delay range of 0-127.5 ns and 0.5 ns step (Fig. 2). Thus, the total delay range of the OPDM is 128 ns.
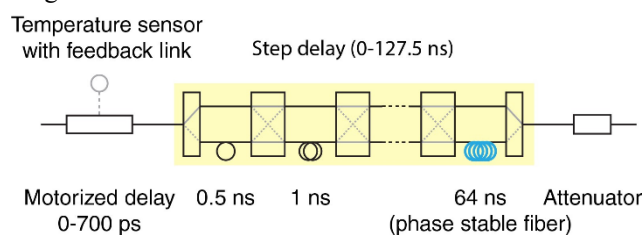
Figure 2: OPDM layout.

The step delay is based on full 2x2 optical switches (Fig. 2). Such a design provides lower total insertion delay compared to using 1x2 switches and lower insertion loss than the solution, where 2x2 switches are used as a single bits by short-circuiting the crossed outputs. The higher bit delays are implemented using phase-stable optical fiber to reduce temperature dependence [3]. To minimize the total insertion loss all switches have been carefully selected to have the lowest possible losses for all passages, resulting in an average insertion loss per switch of ~0.2 dB. The resulting OPDM total insertion loss is less than 5.5 dB. To reduce the intrinsic delay, the switches are mounted in a circular or spiral arrangement, so that can could be spliced as close as possible to each other, providing a total device latency of 14 ps.

THPOSRP07

H0 DIAGNOSTICS FOR THE ELENA ELECTRON COOLER

G. Tranquille[†], CERN, Geneva, Switzerland

Abstract

In addition to antiprotons, the ELENA ring at CERN can also inject protons and H⁻ ions from a dedicated ion source located close to the ring. These particles offer the possibility for extra diagnostics for detailed investigations into the cooling process at the very low energy of the ELENA ring. To this effect a monitor was installed downstream of the electron cooler to measure the recombination of protons with the cooling electrons. Although protons have never been used in ELENA, H⁻ ions are routinely used to setup and optimise the ring. The installed device is now used to monitor the stripping of the H⁻ ions on the residual gas and in the presence of electrons generated by the cooler, providing some insight on the evolution of the beam size during the deceleration cycle and the performance of the electron cooler on the two cooling plateaus.

INTRODUCTION

During the cooling process the centre of mass energy difference becomes very small and ions can capture an electron by radiative or di-electronic recombination. In the next bending magnet, their trajectory becomes very different from that of the circulating ions. For proton beams, neutral hydrogen atoms are formed and travel straight towards a detector.

The formation rate is related to the effective temperature of the electrons and is given by:

$$R_H = N_p \eta \alpha_r n_e \gamma^{-2}$$

where η is the ratio of cooling length to ring circumference, N_p the number of stored ions, n_e the electron current density and α_r the recombination coefficient [1]. Hence the measurement of this rate provides important information on the apparent temperature of the electron beam in the region defined by the overlap with the ions and the possible misalignment of both beams as the highest down-charge rate corresponds to the best matching of electron cooling. Direct measurement of the cooling time and the equilibrium emittances can also be estimated by observing the neutral beam profile.

In ELENA [2] a dedicated H⁻ linac, operating at an energy of 100 keV allows the machine to be operated with H⁻ ions or protons when it is not sending antiprotons to the experiments. Unfortunately, proton mode of operation has never been tested due to the complexity of changing the magnetic polarity of the ELENA ring resulting in a lengthy setting up. Moreover, after such a change, the machine performance in antiproton mode would need much time to recover because of the hysteresis of the magnets.

DETECTOR SETUP

To measure the neutral hydrogen beam profile a detector was installed in the vacuum extension of the 90° bending magnet approximately 6.3 m downstream from the electron cooler. The beam profiler consists of a chevron mounted micro-channel plate (MCP) coupled to a P43 phosphor screen. The H0 atoms that are created travel straight towards the monitor and as they hit the MCP surface, electrons are produced and are amplified in the MCP before they are accelerated onto the phosphor screen. The image of the phosphor screen is acquired by a Raspberry Pi4 computer using the Pi HQ camera mount with interchangeable lenses (see Fig. 1) [3].
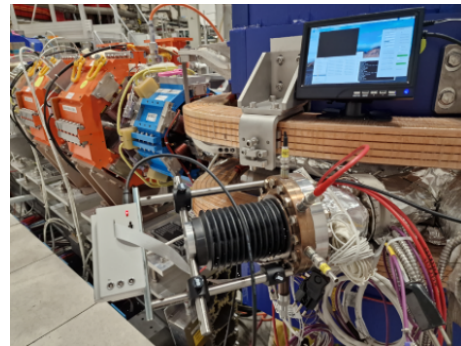
Figure 1: H0 beam monitor in the magnet extension.

Controls and Data Acquisition (DAQ)

The high voltage for the MCP and P43 screen is provided by an iSeg THQ dual channel power supply. A Python script controls the voltage ramp that is applied to the MCP and screen. Camera control is also performed via a Python script which enables the user to adjust the camera settings (resolution, exposure etc.) and to select the acquisition mode (see Fig. 2). Continuous, single/multi frame and video capture are available and can be triggered synchronously with events in the ELENA magnetic cycle.
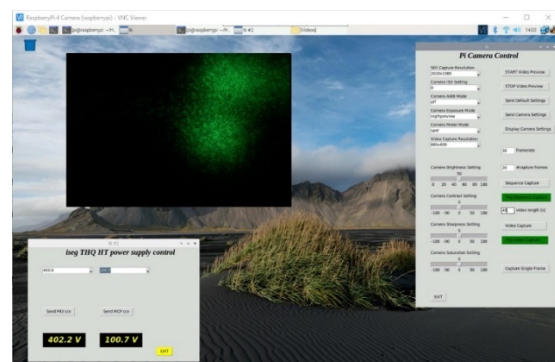
Figure 2: Raspberry Pi controls and DAQ setup.

Calibration

The 12.3-megapixel CCD camera allows single image capture resolutions up to 4056x3040 pixels and a maximum video resolution of 1920x1080 pixels (1080p). A transparent target was mounted on the window and the images at the available video resolutions were acquired to

---

† email Gerard.tranquille@cern.ch

DEVELOPMENT OF A FIELD EMISSION ELECTRON GUN FOR LOW ENERGY ELECTRON COOLING

E.-S. Welker[1], J.Cenede, B. Galante[2], G.A. Tranquille*, CERN, Geneva, Switzerland
[1] also at Technische Universität Wien, Vienna, Austria
[2] at Paul-Scherrer-Institut, Zürich, Switzerland

Abstract

The use of carbon nanotubes (CNT) as a cold electron source for a low energy electron cooler has been studied in detail. To fully characterise different CNT arrays (conditioning process, emitted current, lifetime) and to investigate the optimum electrical configuration of the source to be used in an electron gun, a cold cathode test bench (CCTB) has been set up. From the measurements performed on the CCTB, an electron gun has been designed, constructed and is being tested to measure the properties of an electron gun using a larger (4 cm diameter) CNT array as the source. The CCTB has been modified to incorporate a beam transport system as well as the relevant diagnostics needed to perform the experiments. The results will be compared to the CST Particle Studio simulations and will be used to optimise the design for use in the ELENA low energy electron cooler.

INTRODUCTION

In ELENA (Extra Low Energy Antiproton Ring), electron cooling is fundamental to reduce the emittance blow-up of the antiproton beam so that a focused and bright beam can be delivered to the experiments [1]. Presently, the electron gun relies on thermionic emission, where a tungsten-doped barium oxide (BaO) source is heated to 1200 °C. However, this imposes several limitations on the transverse beam energy and the required magnet system. A cold emission-based electron gun might overcome these constraints, as field emission relies solely on high electric fields to both generate and control the electron beam.

Carbon Nanotubes (CNTs) are considered among the most promising materials for this purpose, and their feasibility as field emitters has been studied. Previous research [2] established CNT cathodes as viable candidates for the use in the electron cooler of ELENA. Still, there remains a crucial research gap in determining their optimal characteristics (maximal current density, lifetime, etc.). Bridging this gap is fundamental for advancing the development of a more efficient electron gun system in ELENA, especially in light of the requirements of future particle accelerators.

EXPERIMENTAL SET-UP

The gun assembly was installed in a vacuum tank to enable an Ultra-High Vacuum (UHV) environment and mounted on a specifically constructed Cold-Cathode-Test-Bench 2 (CCBT2).

Gun Description

The CNT-based gun prototype (see Fig. 1) is comprised of a sample holder with a 4 cm x 4 cm hollow well to place the CNT-Sample. Vertically aligned Carbon Nanotube (VCNT) arrays have been shown to have the most optimal emission properties for our purposes [2]. The VCNTs were grown on silicon plates by using chemical vapor deposition. The gun also features two finely conductive grids, made out of a highly n-doped silicon wafer with a mesh pattern (15 μm square holes with 3 μm walls). The first grid acts as a extracting anode by developing a local electric field, while the second grid is used to decelerate the beam. For insulation between the elements and to limit the beam size, two MACOR® rings are employed. The final component is an aluminium ring with a triangular-shaped cross-section, essential for maintaining straight field lines and keeping the transverse energy of the emitted beam low.

Einzel-Lenses

Given the considerable drift distance between sample and detector, an Einzel-Lens system (comprised of three cylindrical and symmetric electrodes) is used to transport and focus the beam onto an imaging screen. The configuration of voltages determines the fringe fields and thus how the particles will be deflected and focused - without significantly changing their kinetic energy. Typically, the outer electrodes share a common electrical potential, while the central electrode is held at a different potential. It was decided to use the lenses in the acceleration-deceleration mode, as this mode is preferable for longer focal lengths due to the minimized spherical and chromatic image aberration [3].
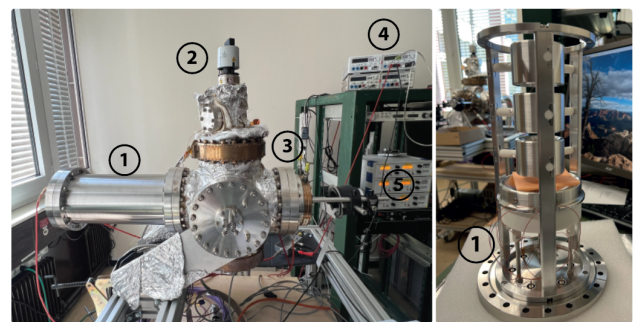
Figure 1: Left: Cold-Cathode-Test-Bench 2: ① Vacuum tank with gun assembly ② Pfeiffer Vacuum Dual Gauge ③PHOTONICS Ion Beam Profiler HM6012 Multimeter ⑤ ISEG HV Power Supply, Right: CNT-based gun assembly.

---

* gerard.tranquille@cern.com

INVESTIGATION OF ION TRAPPING AND BEAM-INDUCED FLUORESCENCE AT THE ELECTRON COOLER TEST-BENCH AT HIM*

T. Beiser[†1], K. Aulenbacher[1], J. Dietrich, Helmholtz-Institute Mainz, Germany
and GSI Helmholtzzentrum für Schwerionenforschung, Darmstadt, Germany
[1]also at Johannes Gutenberg-University, Mainz, Germany

Abstract

Beam-current dependent and wavelength-resolved studies of the beam-induced fluorescence at the electron cooler test-bench recorded with a low-noise, cooled sCMOS-camera, will be presented. As a new feature, a high-voltage switch was utilized for beam interruptions, counteracting ion trapping.

BEAM-INDUCED FLUORESCENCE AT THE ELECTRON COOLER TEST BENCH AT HIM

The test bench uses an energy-recovery setup to produce an electron beam [1] with up to 1 A of 30 keV electrons for 3 kW of wall power (see Figure 1). Beam-induced fluorescence (BIF) was observed in the residual gas of the beam pipe at 3×10^{-10} mbar (see Figure 2). Most measurements were taken with 18 keV electrons and a current of 550 mA to limit the X-Ray exposure of the cooled, low-noise sCMOS camera. Images were acquired over 30 s, with a 400–550 nm bandpass filter to limit the black-body background generated by the thermionic cathode [2]. The resulting profiles were averaged over 500 pixel rows (see Figure 3).

The observed data showed an intensity increase of the BIF over time, plateauing after 3-5 minutes. This was noticeable even after normalizing for the change in pressure, a result of the collector heating induced by the dumped electrons. Taking this into account and measuring the BIF for a number of beam currents from 0 to 550 mA, a overproportional correlation of the integrated signal intensity with the beam current became evident (see Figure 4). This suggested the trapping of photon-emitting ions.

ION TRAPPING IN THE ELECTRON BEAM

Residual gas particles are ionized by the electron beam along its path. To explain the trapping mechanism, the DC electron beam of the test-bench can be approximated as a cylindrical homogeneous charge distribution. The grounded, small apertures of the anode and the deceleration optics along the beam path shape the beam potential and facilitate longitudinal trapping (see Figure 5), as long as the momentum transfer is small enough. A simple model was derived to explain the shape of the BIF. The measured BIF photons are most likely emitted by trapped ions that get excited by
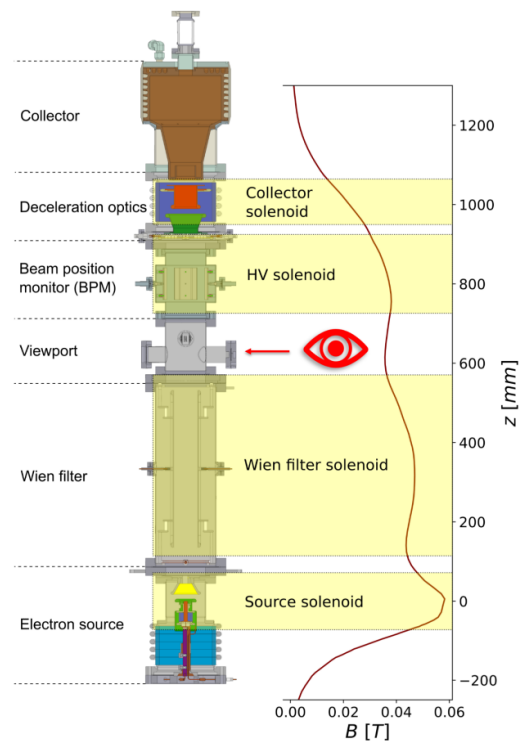
Figure 1: Schematic of the test bench with the simulated solenoid field-strength along the beam path.
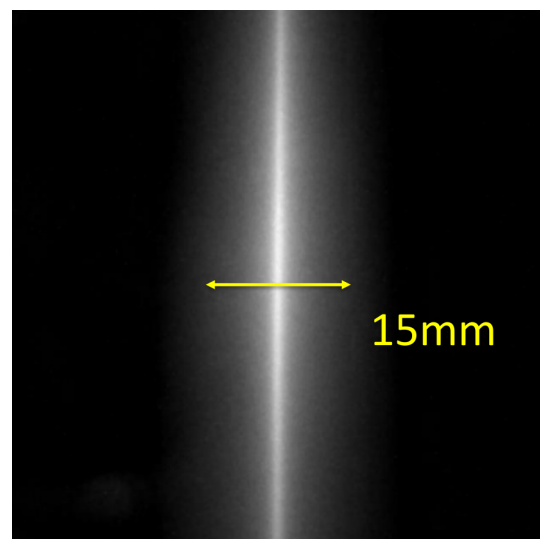
Figure 2: Image of BIF produced by a 30 keV, 1 A electron beam with indicated width.

JSPEC: A PROGRAM FOR
IBS AND ELECTRON COOLING SIMULATION*

H. Zhang†, Y. Zhang, S.V. Benson, M.W. Bruker
Thomas Jefferson National Accelerator Facility, Newport News, VA, United States

Abstract

JSPEC (JLab Simulation Package on Electron Cooling) is an open-source C++ program developed at Jefferson Lab to simulate the evolution of the ion beam under the intrabeam scattering effect and/or the electron cooling effect. JSPEC includes various models of the ion beam, the electron beam, and the friction force, aiming to reflect the latest advances in the field and to provide a useful tool to the community. JSPEC has been benchmarked against other cooling simulation codes and experimental data. It has been used to support the cooler design for JLEIC, an earlier JLab design for the Electron-Ion Collider. A Python wrapper of the C++ code, pyJSPEC, for Python 3.x environment has also been developed and released. It allows users to run JSPEC simulations in a Python environment and makes it possible for JSPEC to collaborate with other accelerator and beam modeling programs, as well as plentiful Python tools in data visualization, optimization, machine learning, *etc*. A Fortran interface is being developed, aiming at seamless call of JSPEC functions in Fortran. In this report, we introduce the features of JSPEC, with a focus on the latest development, and demonstrate how to use JSPEC, pyJSPEC, and the FORTRAN interface with sample codes.

INTRODUCTION

Intrabeam scattering (IBS) [1] is an effect that may reduce the quality of a high-intensity beam and impair the luminosity of a collider. Electron cooling [2] is an experimentally proven leading method to reduce the ion beam emittance and it is often used to mitigate the IBS effect. JSPEC (JLab Simulation Package on Electron Cooling) is an open-source program [3] developed at Jefferson Lab, which simulates the evolution of the ion beam under the influence of both IBS and electron cooling effects. Originally developed to support the Electron Ion Collider (EIC) design at Jefferson Lab [4], our goal is now to provide a convenient toolkit for the IBS and electron cooling effect simulation to the wider accelerator community. JSPEC includes the most frequently used formulas for the friction forces and variant models of electron/ion beams. The main code is developed in C++ with emphasis on both the validity of the physical models and the efficiency of computation. Most modules in JSPEC supports parallel computing in shared-memory structure using OPENMP. A Python wrapper, pyJSPEC, gives users access to most JSPEC functions in Python 3.x environment allowing JSPEC to work collaboratively with other simulation tools that have a Python interface [5, 6]. Many legacy codes, developed in

Fortran, remain widely used in accelerator modelling. In response to this, we are developing a Fortran interface for JSPEC. Our goal is to allow JSPEC functions to be seamlessly called within Fortran, facilitating the modelling of the electron cooling effect in those codes.

FEATURES

The basic feature of JSPEC is to calculate the emittance growth rate of the ion beam under the IBS and/or the electron cooling effect. The rate at time t is defined as $r_i(t) = \frac{1}{\epsilon_i(t)} \frac{d\epsilon_i(t)}{dt}$, where $i = x, y, s$, representing the horizontal, vertical, and longitudinal direction, and ϵ_i is the emittance in the respective direction. For the IBS rate, JSPEC provides the Martini model [7], the original Bjorken-Mtingwa model [8] calculated by Nagaitsev's method [9], and the complete Bjorken-Mtingwa model with vertical dispersion and non-relativistic terms included [10]. The electron cooling rate is calculated statistically on a group of sample ions, each receiving a *kick* by the friction force. The rate is calculated as the relative change of the emittance per unit time before and after the kick. JSPEC provides several formulas [11-14] for both the non-magnetized and the magnetized friction force. Using different formulas in the transverse and the longitudinal direction is allowed.

JSPEC also simulates the evolution of the ion beam under the IBS effect and/or the electron cooling effect. The RMS dynamic model represents the ion beam by its macroscopic parameters, *i.e.* the emittances, the momentum spread, and the bunch length (for a bunched beam), calculates the instant expansion rate r at a time t and updates the parameters using $\epsilon_i(t + \Delta t) = \epsilon_i(t) \exp(r_i \Delta t)$ for the time step Δt. The particle model applies kicks due to IBS and electron cooling to sample ions and moves them by a random phase advance for the betatron and synchrotron oscillation in Δt. The turn-by-turn model is similar to the particle model but the betatron and synchrotron motion is modeled by a linear transfer matrix and the simulation is carried out in a turn-by-turn manner.

Recently we have added two new features [15]. One is to treat the cooler as a lengthy element. Previously, JSPEC used a thin lens model for the cooler. The electron beam is assumed constant during the cooling process. In the new model, we cut the cooler into n slices. For ions, each slice works as a drift. The position of an ion changes but the velocity does not when moving through a slice. In the middle of the slice, the ion get a kick due to cooling. For cooling simulations, it is not necessary to consider the motion of individual electrons but rather the properties of the electron beam as a whole. For non-magnetized beam, we calculate the Twiss function β and α at different locations and then

INFLUENCE OF ENERGY SHIFT OF ELECTRON BEAM ON THE ELECTRON COOLING AT EicC*

X. D. Yang†, Institute of Modern Physics, CAS, Lanzhou, China

Abstract

The cooling process of 20GeV proton beam was simulated in the case of different energy shift of electron beam. The changes of horizontal emittance and longitudinal momentum spread of proton beam with time was presented. The different performances in horizontal and longitudinal direction were observed comparing with the traditional low energy electron cooling. The final emittance and minimum momentum spread was demonstrated in the different parameters configuration. In order to achieve expected cooling requirements, the energy shift of electron beam should be paid enough attention in the case of high energy electron cooling, especially considering a RF accelerator as electron cooling device.

INTRODUCTION

The basic requirement of electron cooling is that the longitudinal average velocity of the electron beam is equal to that of the ion beam. In order to ensure the desired cooling effect, the energy of the electron beam should be set precisely and accurate matching of longitudinal velocity of the ion beam [1, 2].

The deviation of electron beam energy from the optimal value reflects two requirements. On the one hand, the energy of an electron beam needs to be measured accurately in the electron cooling commissioning and operation. On the other hand, in order to meet the parameters required for cooling, the energy stability and energy spread of the electron beam are required in the design and manufacture of electronic cooling devices.

In future projects, electron cooling plays an important role. It is a necessary means to obtain high brightness and long lifetime ion beams. The performance of electron cooling is related to many parameters, such as ion beam, electron beam, storage ring, electron cooling device, etc. The energy shift of the electron beam is an important indicator. The effects of energy shift of electron beam on the transverse and longitudinal cooling processes should be simulated previously. In particular, the effect on longitudinal cooling, the simulation results have reference value for the design and operation of electron cooling devices in the future.

The electron cooling time not only depends on the lattice parameters of the storage ring, the Betatron function, dispersion of the cooling section, such as energy, initial emittance and momentum spread of proton beam, but also on the construction parameters of electron cooling device, the strength of magnetic field, the parallelism of magnetic field in the cooling section, the effective cooling length, and the parameters of electron beam, such as radius, density and temperature of electron beam. These parameters are determined by the storage ring and the technology limitation, on the other hand, they are influenced and restricted each other.

The performance of electron cooling is not only related to the ion beam parameters of the storage ring, but also related to the electron beam parameters of the electron cooling device. The important parameters of the electron beam are the transverse and longitudinal temperature of the electron beam.

The electron cooling process of 20 GeV proton beam in EicC was simulated in cases of variety of parameters in the previous studies [3, 4], the longitudinal temperature of the electron beam was not involved in the simulations. The energy shift of the electron beam was not taken into account.

During the optimization of electron cooling process, the average velocity of an electron and an ion is required to be equal. In the case of the given distribution of the ion beam, the energy spread of the ion beam is about the same order of magnitude comparing with the electron beam.

The energy shift of the electron beam is a very important parameter in the electron cooling process, especially in high-energy electron cooling [5, 6]. And the energy shift of the electron beam determines the final parameters of the proton beam after electron cooling, so the effect of energy shift of electron beam on electron cooling is necessary.

The RF accelerator is the option for high-energy electron cooling [7, 8]. The electron beam generated by the RF accelerator has a large energy spread. The necessary measures are needed to reduce the energy spread of the electron beam.

From the experience and experimental results from LEReC BNL [9-11], the longitudinal temperature of the electron beam should be paid enough attention in the case of high energy electron cooling.

The influence of electron beam energy shift on electron cooling process should be investigated. It is useful to understand the requirements for electron cooling, and provide the guidance for design parameters of high energy electronic cooling.

MOTIVATION

In order to get the required brightness in the future EicC project, not only does it require an intense proton beam, but also it requires a small emittance and momentum spread. Electron cooling can increase the density of phase space and improve the quality of proton beam, Electron cooling plays an important role.

In the second phase of EicC, the energy of proton will upgrade to 60~100 GeV, and the energy of electron beam will increase to 5~10 GeV, the luminosity will expect to achieve 1×10^{35}.

DEVELOPMENT OF AN ERL FOR COHERENT ELECTRON COOLING AT THE ELECTRON-ION COLLIDER

K. Deitrick*, S. Benson, Thomas Jefferson National Accelerator Facility, Newport News, VA, USA
J. Conway, B. Dunham, R. Eichhorn, C. Gulliford, V. Kostroun,
C. Mayes, K. Smolenski, N. Taylor, Xelera Research LLC, Ithaca, NY, USA
W. Bergan, A. Fedotov, D. Kayran, E. Wang, D. Xu, Brookhaven National Lab, Upton, NY, USA
N. Wang, Cornell University, Ithaca, NY, USA

Abstract

The Electron-Ion Collider (EIC) is currently under development to be built at Brookhaven National Lab and requires cooling during collisions in order to preserve the quality of the hadron beam despite degradation due to intra-beam scattering and beam-beam effect. An Energy Recovery Linac (ERL) is being designed to deliver the necessary electron beam for Coherent electron Cooling (CeC) of the hadron beam, with an electron bunch charge of 1 nC and an average current of 100 mA; two modes of operation are being developed for 150 and 55 MeV electrons, corresponding to 275 and 100 GeV protons. The injector of this Strong Hadron Cooler ERL (SHC-ERL) is shared with the Precooler ERL, which cools lower energy proton beams via bunched beam cooling, as used in the Low Energy RHIC electron Cooling (LEReC). This paper reviews the current state of the design.

INTRODUCTION

The Electron-Ion Collider (EIC) is a partnership project between Brookhaven National Lab (BNL) and Thomas Jefferson National Accelerator Facility (TJNAF) to be constructed at BNL, using much of the existing infrastructure of the Relativistic Heavy Ion Collider (RHIC); a layout of the EIC is shown in Fig. 1. Collisions occur between the hadrons in the Hadron Storage Ring (HSR) and the electrons supplied by the Electron Storage Ring (ESR); in order to maintain a high average polarization of the ESR, bunches are frequently replaced using the Rapid Cycling Synchrotron (RCS). While most of the magnets for the HSR are repurposed RHIC magnets, already installed in the existing tunnel, both the ESR and RCS will have to be installed. In the current scope of the EIC, only one interaction region (IR) is supported, sited at the current IR6 of RHIC; however, it is highly desired that a second IR may be supported at IR8 in the future, and design efforts support that eventuality [1].

In order to achieve the design emittances of the hadron beam, a two-stage cooling system is necessary. First, hadron beams are injected into the HSR and cooled to the target emittances. After the target emittances are achieved, the HSR is ramped to the collision energy, and the hadron beam is cooled during collision in order to maintain the beam emittances; preserving the design emittances is critical to achieve the desired luminosity of the EIC. The electron cooler which provides cooling to the hadron beam is located in IR2 [1].

---

* kirstend@jlab.org

Figure 1: The current layout of a portion of the Electron-Ion Collider (EIC). The Hadron Storage Ring (HSR), Electron Storage Ring (ESR), and the Rapid Cycling Synchrotron (RCS) labels are color-coded to their respective rings; the current and proposed IRs are shown at IR6 and IR8, with the electron cooler in IR2.

COOLING MECHANISMS

The two cooling stages use different cooling mechanisms in order to cool the hadron beam. The Pre-cooler, which cools during injection, uses non-magnetized bunched beam cooling, which is the mechanism currently used in Low Energy RHIC electron Cooling (LEReC) [2, 3]. In this scheme, three electron bunches at an energy of 13 MeV are used to cool each hadron bunch, which has an energy of 24 GeV.

The Strong Hadron Cooler (SHC), which cools during collision, uses Coherent electron Cooling (CeC) where the electron beam detects the hadron distribution, amplifies the imprinted distribution, and feeds back on the hadron beam to reduce the emittance of the hadron beam [4]. The cooling section of the SHC can be separated into three sections for each of these actions - modulator, amplifier, and kicker, respectively. The type of CeC to be used is microbunched electron cooling (MBEC), where chicanes and space charge provide the necessary amplification. While the EIC is intended to operate over a range of proton energies, only the 275 and

SIMULATION STUDY OF A MULTI-STAGE RECTILINEAR CHANNEL FOR MUON COOLING

R. H. Zhu[1*], J. C. Yang, H. Zhao

Institute of Modern Physics, Chinese Academy of Sciences, Lanzhou, China

C. T. Rogers, Rutherford Appleton Laboratory, Didcot, United Kingdom

[1]also at University of Chinese Academy of Sciences, Beijing, China

Abstract

The muon collider has the potential to be a powerful tool for the exploration of frontiers in particle physics. In order to reach the high luminosity, the 6D emittance of the muon beam needs to be reduced by several orders of magnitude. Ionization cooling, which has recently been demonstrated in 4D by the Muon Ionization Cooling Experiment (MICE), is a promising cooling method for the muon beam. In the future, muon production and 6D ionization cooling experiments are planned at the High Intensity Accelerator Facility (HIAF) at the Institute of Modern Physics, Chinese Academy of Sciences (IMP, CAS). In this paper, a multi-stage rectilinear 6D ionization cooling channel is developed and the cooling simulation results using G4Beamline are presented, indicating good performance for muon beams with large emittance. This work serves as a good starting point for future research at HIAF.

INTRODUCITON

Electron (e+e-) colliders have many advantages over hadron colliders mainly because they produce much cleaner and simpler collision events, allowing physicists to analyze the resulting particles more easily. However, the multi-TeV collision energy is hard to achieve for (e+e-) colliders due to the small mass of the electron which will lead to the significant radiative energy loss. Muons have much larger mass compared with electrons which makes them almost not affected by the synchrotron radiation. Meanwhile, muons also have electron like nature, thus it seems wiser and more cost effective to choose muon colliders for high-energy physics study [1].

One technical challenge for the muon collider is that the muon beam emittance from the pion decay is too large which significantly exceeds the acceptance of the downstream accelerator parts and a dedicated cooling channel is needed to shrink the beam volume space [2]. A conceptual rectilinear cooling channel containing 12 stages has been designed during the MAP (muon accelerator program) project. Its basic idea is using stronger focus for the later stage to achieve better transverse cooling and tilting the solenoid coils to generate dispersion for longitudinal cooling. However, tilting the solenoid might have technical issues. So, using extra dipole magnet for dispersion generation might be a better choice. Here we present a multi-stage rectilinear cooling channel design with additional dipole magnets which shows

_____

* zhuruihu@impcas.ac.cn

a better cooling performance compared with the design of previous studies and this conceptual design of rectilinear cooling channel would be a preparation work for the muon cooling experiments at HIAF [3] in the future, as shown in Fig. 1.
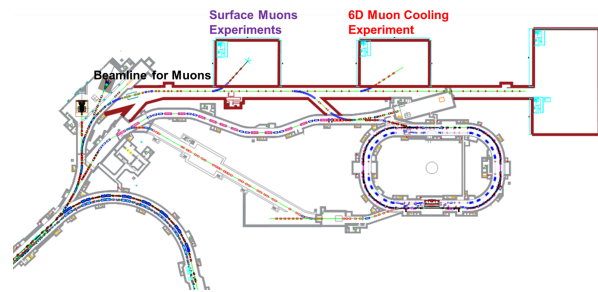
Figure 1: Muon Experiments Planned at HIAF.

DESCRIPTION OF RECTILINEAR COOLING LATTICE DESIGN

Formulas of Ionization Cooling

Ionization cooling involves muon beams losing both transverse and longitudinal momentum by the ionization of the atoms in the absorber material. The longitudinal momentum will get compensated in the RF cavities and the transverse momentum will not. Thus the momentum of the muons is more parallel and the emittance is reduced. The emittance evolution neglecting energy straggling is decribed as [4]:

$$\frac{d\epsilon_n}{ds} = -\frac{1}{\beta^2}\frac{dE_\mu}{ds}\frac{\epsilon_n}{E_\mu} + \frac{1}{\beta^3}\frac{\beta_T(13.6\text{ MeV})^2}{2E_\mu m_\mu c^2 L_R} \quad (1)$$

where ϵ_n is the normalized transverse emittance, E_μ is the muon beam energy in GeV, m_μ is the muon mass, β is the muon particle velocity, c is the speed of light, β_T is the transverse beta value, dE_μ/ds is the energy loss per unit length and L_R is the radiation length of absorber material. The first part of this equation can be regarded as cooling term and the second heating term. The equilibrium transverse emittance is defined when dE_μ/ds in Eq.(1) is 0 [4]:

$$\epsilon_{n,eq} = \frac{\beta_T(13.6\text{ MeV})^2}{2\beta m_\mu c^2 L_R|\frac{dE_\mu}{ds}|}. \quad (2)$$

It can be easily seen from the Eq. (2) that, to reach a lower equilibrium transverse emittance, the focusing at the

BEAM MEASUREMENTS OF A PALMER PICK-UP
FOR THE COLLECTOR RING OF FAIR

C. Peschke*, R. Böhm, C. Dimopoulou, S. Wunderlich, C. Zhang, GSI, Darmstadt, Germany

Abstract

The stochastic cooling system of the **C**ollector **R**ing (CR) of the future FAIR facility will have three **p**ick-**u**p (PU) tanks and two kicker tanks. For the pre-cooling of very hot RIBs, a pick-up tank with eight Faltin-type structures for Palmer-cooling has been constructed by GSI. The structures have been designed using **H**igh-**F**requency **S**tructure **S**imulator (HFSS).

The Palmer PU tank has been tested with $\beta = 0.83$ proton beams at the **Co**oler **Sy**nchrotron (COSY) of the FZJ. This publication presents the results of measurements with beam and compare them with simulations (HFSS and Microwave Studio).

The pick-up operates at room temperature. But it has artificial cold loads instead of normal terminators. The results of the noise temperature measurements are also be presented.

PALMER PICK-UP

For very hot rare isotope beams, the distance from the slotline pick-ups to the kickers is too large. The undesired mixing prevents cooling. Therefore a Palmer pick-up with smaller distance to the kicker permits an high acceptance for the start of the cooling cycle.
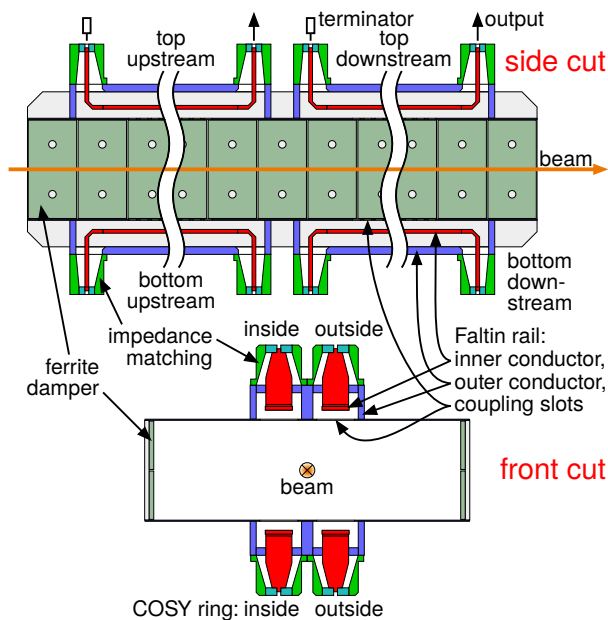
Figure 1: Layout of the Palmer pick-up tank.

Figure 1 shows the schematic layout inside the palmer pick-up tank. It uses Faltin type structures for coupling and

---

* C.Peschke@gsi.de

has been developed using HFSS FEM field calculation program [1]. Faltin rails show an high dispersion. To archive an octave bandwidth the four long rails of the Palmer arrangement, the rails are divided into identical upstream and downstream parts. A lot of ferrite material (Ferroxcube 4S60) has been installed to damp undesired wave modes. The dampers are on the side walls, far from the coupling slots, to avoid reduction of the shunt impedance.

MEASUREMENT SETUP

To verify the design performance, the CR Palmer pick-up tank has been installed in the COSY ring, as shown in Fig. 2. We have used stored proton beams for our experiment. The beams were weakly bunched to allow the **b**eam **p**osition **m**onitors (BPM) to work. Table 1 shows the parameters typically used here.
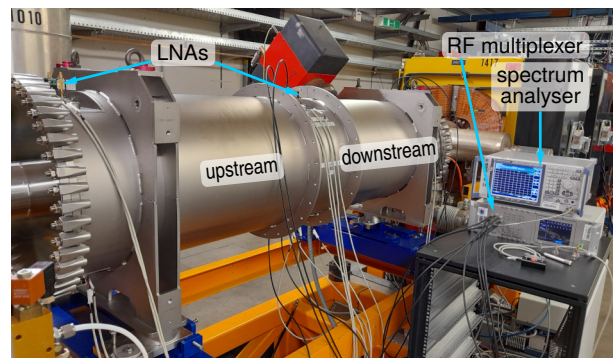
Figure 2: CR Palmer pick-up tank installed in COSY ring.

Table 1: Typical Beam Parameters

velocity factor	$\beta = 0.830$
number of protons	$N = 1.7 \cdot 10^{10}$
(measured for each run)	
beam dimensions	$\Delta x = 5.3$ mm
	$\Delta y = 3.9$ mm
dispersion at Palmer-PU	$D = 0$ m
RMS momentum spread	$\Delta p/p = 2.2 \cdot 10^{-4}$

For the measurements, the tank has been equipped with all eight Faltin rails and the low noise amplifiers (LNAs), but without the subsequent Palmer signal processing. Figure 3 shows a block diagram of the measurement setup.

To prevent additional noise from cable damping, the low noise amplifiers (LNAs) were installed directly on the vacuum feedthroughs. The LNAs at the outputs of the Faltin rails were used as normal amplifiers for the Schottky signals.

HOW TO ADJUST STOCHASTIC COOLING SYSTEMS

N. Shurkhno†, GSI, Darmstadt, Germany

Abstract

The paper summarizes techniques and algorithms for adjustment of stochastic cooling systems, that have been developed and tested at the COSY accelerator facility (FZ Jülich, Germany). An overall goal was to automate typical time-consuming manual adjustment routines. As a result, a set of algorithms based on a theoretical description of the stochastic cooling process has been developed, which allows accurate and fast automatic adjustment of main system's parameters. The methods have been elaborated and used at COSY during development and testing of stochastic cooling systems for HESR and are planned for further use at the FAIR accelerator complex (GSI, Germany). The methods are quite universal and can be applied or adapted to any similar system.

INTRODUCTION

In a broad sense, an adjustment of a stochastic cooling system is bringing its broadband frequency response to its instantaneous optimum, so that it would provide the fastest cooling at a given moment of time. From a hardware point of view, common parameters for adjustment are system gain and delay and optionally a comb filter if it is used. System gain and delay control the amplitude and phase slope of the system frequency response respectively. The developed adjustment techniques for both gain and delay are based on calculating the system transfer function from open loop measurements and using it in Focker-Planck or single particle equations to obtain the optimum values, while the comb filter is adjusted iteratively. The system delay and comb filter adjustment algorithms are fully automatic, accurate and robust, providing adjustment time ~1 s or less, whereas previous manual adjustment could easily take hours. System gain adjustment on the other hand, is more subtle within the developed approach, allowing simple adjustment only in special cases (negligible hardware noise and IBS, non-resonant BTF), while generally requiring additional measurements and elaboration. The adjustment techniques have been developed and tested at the COSY accelerator facility (FZ Jülich, Germany) as a part of the HESR stochastic cooling systems development (GSI, Germany) [1].

SYSTEM TRANSFER FUNCTION

System transfer function can be estimated or directly calculated from open-loop measurements (OLM), which is a common technique for studying beam and system transfer functions [2, 3]. Open-loop measurements are made by opening the cooling loop to feed the signal from the vector network analyzer in and out (Fig. 1).

To get a broadband frequency response open-loop measurements should be performed at the full system bandwidth. This is done by measuring multiple single Schottky bands in the passband (single band OLM) or by performing single broadband measurement with VNA sweep points set to the centers of Schottky bands or betatron sidebands (broadband OLM). The single band OLM is very flexible and reliable, it may require some additional processing (e.g., smoothing and correlation with measured particle distribution function). On the other hand, broadband OLM is a single measurement and therefore much faster, but it may produce false results, since it measures only a single point within the Schottky band, which can be influenced, e.g., by a resonance. Also, a combination of methods can be used for cross-checking in an automated setup, preserving measurement speed and identifying possible problems at the same time.
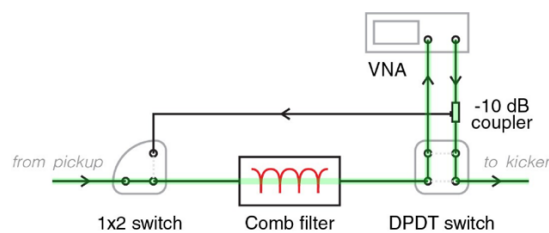
Figure 1: Layout for OLM (green) and comb filter adjustment. To open and close the loop a transfer (DPDT) switch is used, providing the lowest possible insertion delay.

Open-loop measurements produce direct product of beam and system transfer functions, so the latter can be obtained by substituting the BTF in the equation $G(f) = OLM(f)/BTF(f)$, where $G(f)$ and $BTF(f)$ are system and beam transfer functions respectively, f – measurement frequency. Analytical formulas for beam transfer functions are well known and can be found for example in [3, 4].

The overall calculation is reasonably tolerable to measurement uncertainties (beam intensity, particle distribution function, resonances, etc.), since further calculations do not require high accuracy of the system transfer function, as will be discussed later.

The obtained system transfer function is used then for calculating the optimum gain and delay with Fokker-Planck and/or single particle equation in the following form [5]:

$$\frac{dx}{dt} = F(x,t) + \frac{D(x,t)}{x}, \tag{1}$$

where $F(x,t)$ and $D(x,t)$ are drift and diffusion terms (or cooling and heating terms), x is a parameter being cooled.

Single particle equations are often sufficient since we are mostly interested in instantaneous values and not in the cooling evolution.

SYSTEM DELAY ADJUSTMENT

The system delay synchronizes the correction signal with the measured particles. It defines the phase slope of the system transfer function, so a common approach to setting the system delay is to flatten the phase of the OLM and then fine-tune. The delay corresponding to the flattened

EXPERIENCE WITH BEAM TRANSFER FUNCTION MEASUREMENTS FOR SETTING-UP THE STOCHASTIC COOLING SYSTEM IN THE CERN ANTI-PROTON DECELERATOR (AD)

S. Rey*, W. Höfle†, W. Bastos, F. Caspers, B. Dupuy, D. Gamba, R. Louwerse
CERN, Geneva, Switzerland

Abstract

Beam transfer function measurements have regularly been used to set-up the adjustable parameters for stochastic cooling systems. We report on the automation of these measurements at CERN that permit efficient set-up of the cooling loops in the anti-proton decelerator (AD) and enables insight into the bandwidth (nominal frequency range of 850 MHz to 1.7 GHz) of the overall system for the longitudinal, horizontal and vertical cooling at the two different beam momenta of 2 GeV/c and 3.57 GeV/c. Additionally, data collected during machine development sessions can be used to identify areas of improvement and will be indispensable in defining the planned path for consolidation and upgrade of the system. For example, it allows the comparison of the bandwidth with the computed shunt impedance of the currently used kickers. The unwanted crosstalk between the three different planes of cooling is also evaluated and will help to define improvements in the system for the future.

INTRODUCTION

Stochastic cooling is currently used in the CERN Anti-proton Decelerator (AD) at two different beam momenta of 2 GeV/c and 3.57 GeV/c [1]. Anti-protons are routinely decelerated since 1999 [2] and since the start-up after long-shutdown 2 (LS2) exclusively provided for further deceleration to the new ELENA decelerator [3]. The transfer momentum to Elena is 100 MeV/c with electron cooling used at two further momentum plateaus in AD at 300 MeV/c and 100 MeV/c.

In the framework of increasing the efficiency and set-up time of the stochastic cooling system in AD it was highly desirable to conceive an automated beam transfer function measurement that could go beyond the normal setting-up, but also be used for diagnosis during the run, and to probe the efficacy and available bandwidth of the existing systems that operate in all three planes at the two beam momenta. The data collected during such measurements helps to define upgrades required in view of future operation, also possibly with the stochastic cooling used at a lower momenta.

OVERVIEW OF AD STOCHASTIC COOLING SYSTEM AND BEAMS

The stochastic cooling system in AD comprises four elements in the ring: horizontal pick-up UHM 3107, horizontal kicker KHM 0307, vertical pick-up UVM 3207 and vertical

---

* stephane.franck.rey@cern.ch
† wolfgang.hofle@cern.ch

kicker KVM 0407 [1]. The longitudinal cooling is obtained using the same pick-ups and kickers in their common mode combining both signals from the horizontal and vertical pick-ups and splitting on the back-end the signal to feed both the horizontal and vertical kickers through notch filters.
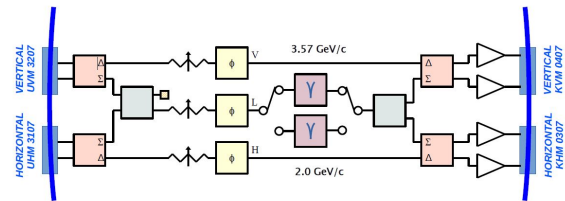
Figure 1: AD Stochastic Cooling Overview.

Layout and Optics for Stochastic Cooling at 2 GeV/c and 3.57 GeV/c

The two pairs of pick-up and and kicker are installed in locations opposing each other in the ring. For a ring circumference of 182.433 m the beam orbit length between pick-up to kicker and kicker to pick-up amounts to between 91.21 m to 91.22 m in length rounded to centimeters for nominal momentum. For the two cooling plateaus (2 GeV/c and
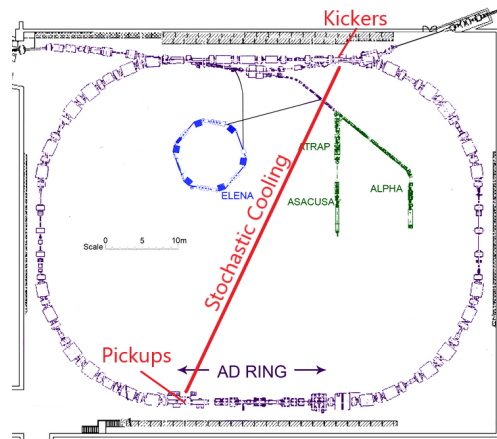
Figure 2: AD Stochastic Cooling.

3.57 GeV/c) the beam β equals 0.90532 and 0.96724, respectively, giving time of flights of ~ 336.1 ns and ~ 314.6 ns. The time of flight difference of ~ 21.5 ns must be properly compensated when switching between the two plateaus. Implementation of the switching is by means of RF relays controlled by a PLC system and with the total delay difference split into several parts located along the signal chain. The pick-ups have only one feed-through per side with internal delays being adjusted for 3.57 GeV/c, while the kicker

KICKER FOR THE CR STOCHASTIC COOLING SYSTEM BASED ON HESR SLOT-RING COUPLERS

R. Stassen†, R. Greven, H. Schneider, J. Wolters, Forschungszentrum Jülich, Jülich, Germany
B. Breitkreutz, GSI Helmholtzzentrum für Schwerionenforschung GmbH, Darmstadt, Germany

Abstract

A 'light' version of the HESR stochastic cooling system was already successfully tested in the Cooler Synchrotron COSY. There the stochastic cooling system was operated together with the original PANDA cluster jet target from University Münster. The system layout includes all components as planned for the HESR like low noise amplifier, switchable delay-lines and optical notch-filter. The robust slot-ring design has been proven. Hence it was decided to use this concept for the CR kicker as well. Therefore, the parameters need to be adapted for the CR cooling system. However, the significantly higher RF power requires a new water cooling concept. First simulations and measurements show that using heat pipes could be a possible solution. At COOL'23 main parameter as well as the promising results achieved at COSY will be presented.

STOCHASTIC COOLING SYSTEM OF HESR

The HESR is the planned High Energy Storage Ring (1.5 - 15 GeV/c) for antiprotons at the FAIR facility (Facility for Antiprotons and Ion Research) in Darmstadt (GSI) [1]. One of the key systems at the HESR will be the stochastic cooling. It is not only essential to enhance the beam quality for the experiments but is also indispensable for the accumulation of antiprotons in HESR [2]. The system is based on dedicated structures. Each beam-surrounding slot of these so-called slot-ring couplers covers the whole image current without a reduction of the HESR aperture [3, 4].
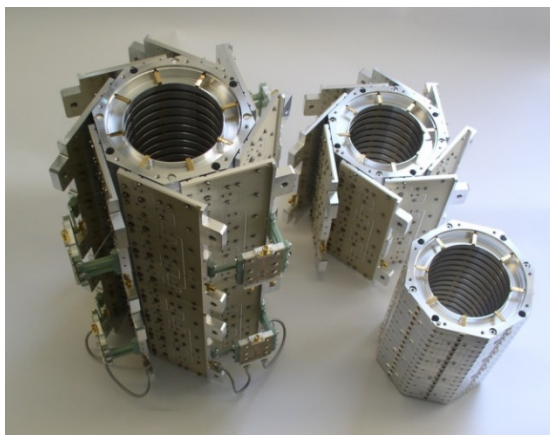
Figure 1: Stacks of slot ring couplers with and without 16:1 combiner-boards and two stacks mounted together including 2:1 combiner with heat-trap.

r.stassen@fz-juelich.de

Each resonant ring structure is heavily loaded with eight 50 Ω electrodes for a broad-band operation. The rings are screwed together to a self-supporting structure in stacks of 16 rings. Four of these stacks will build the spindle for one tank. Figure 1 shows these stacks; one without combiner, one with combiner board and a combination of two stacks including additional 2:1 combiner especially designed to minimize the heat flow to the 16:1 combiners. The structures can be used for all cooling directions simultaneously. No complicate plunging system is needed.

A 'light' cooling version with one original pickup (PU) and kicker (KI) tank of the HESR was installed in COSY. The system layout includes all components as planned for the HESR like low noise amplifiers, switchable delay-lines, optical notch-filter and - of course - the high power amplifier. The inner structure of the pickup was cooled down to less than 20 K within 10 h. Although the tank is not bakeable, the vacuum reached already $1 \cdot 10^{-10}$ mbar. The HESR needs fast transmission-lines between PU and KI. Beside air-filled coax-lines, optical hollow fibre-lines are very attractive [5]. Three of such 50 m long fibres were installed in COSY and used during the cooling experiments. See Fig. 2 below.
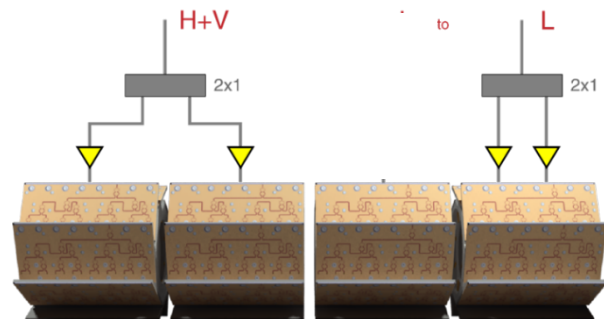
Figure 2: HESR Kicker arrangement at COSY.

The kicker tank was equipped with six custom-made HESR 100 W power amplifier based on gallium nitride (GaN) transistors. Although GaN is not as linear as Gallium Arsenide (GaAs), it is meanwhile the first choice of broadband power amplifier in the GHz region. The kicker is used for all three cooling planes. Two groups of the HESR kicker are for both transverse planes and one group with two amplifiers for longitudinal cooling.

PANDA TARGET MEETS HESR STOCHASTIC COOLING SYSTEM IN COSY

The HESR originally has been optimized for the PANDA experiment (antiProton ANihilation at DArmstadt). The PANDA collaboration comprises more than 500 scientists coming from 20 countries. Their research is dedicated to fundamental physics research covering topics such as

ELECTRON COOLING IN NICA ACCELERATION COMPLEX

A. Butenko, V. Lebedev†, I. Meshkov, K. Osipov, Yu. Prokopjechev, V. Shpakov, S. Semenov,
A. Sergeev, E. Syresin, R. Timonin, G. Trubnikov

Joint Institute for Nuclear Research, Dubna, Russia

M. Bryzgunov, A. Bubley, V. Panasyuk, V. Parkhomchuk, V. Reva

Budker Institute for Nuclear Physics SB RAS, Novosibirsk, Russia

Abstract

The paper reports results of experimental studies of electron cooling carried out during commissioning of injection complex of NICA (the Nuclotron-based Ion Collider fAcility). Further plans of electron cooling developments and usage are also described.

NICA INJECTION COMPLEX

The Nuclotron-based Ion Collider fAcility (NICA) is in construction at JINR [1, 2]. The collider first beam tests are planned for the second half of 2024. The goal of the second stage of NICA project is to provide colliding beams for studies of collisions of heavy fully stripped ions at energies up to 4.5 GeV/u. The injection complex consists of two collider rings supporting head-on collisions in two interaction points and the injection complex [3, 4] which includes linac and two synchrotrons: Booster and Nuclotron. The injection complex is already in commissioning for few years. Stable operation of the complex has been achieved and different ion species were delivered to the BM@N and SRC experiments [5, 6] with slow beam extraction. By present time the ion beams of He, Fe, C [7] and Xe [8] were accelerated in these synchrotrons during four beam runs. With start of collider operation, the injection complex has to support both the collider operation and the fixed target experiments with slow extracted beams. Two particle detectors, a Multi-Purpose Detector (MPD) [9] and a Spin Physics Detector (SPD) [10], are located in two straight sections at the opposite sides of the collider.

The Krion-6T [11] ion source introduced into operation in Run IV will provide the beam of highly multicharged ions. $^{197}Au^{31+}$ and $^{209}Bi^{35+}$ ions are planned to be used in the collider operation. In Run IV (Sep. 2022 – Feb. 2023) we used Xe^{28+}. The same ions are expected to be used at the beginning of collider commissioning. In Run IV about a quarter of the ions extracted from the source had the targeted charge. A typical intensity was about 10^8 ions per pulse for the targeted charge. After electrostatic acceleration to 17 keV/u the beam is accelerated in the RFQ and 2 sections of heavy ion linac (HILAC) [12] to the energy of 3.2 MeV/u. Then the beam is injected into the Booster with single turn injection.

The Booster is a superconducting synchrotron designed to accelerate heavy ions to the energy of 600 MeV/u ($A/Z \approx 6$). At the Booster extraction the ions come through stripping foil where they are fully stripped and then are directed to Nuclotron for further acceleration to 3.9 GeV/u.

The collider design report [3] requires the beam intensity of about 10^9 ions per injection complex pulse with cycle duration of ~4-5 s. The beam extracted from Nuclotron will be injected into collider rings where first it is accumulated in the barrier bucket RF, then bunched and brought to collisions.

The ion xenon beam extracted from Krion-6T had ~5 charge states with the targeted charge state (Z=28) taking about 25%. The peak of total ion beam current at the RFQ exit is about 200 μA (curve 1, Fig.1). Since there is considerable loss for the non-target states the total beam current is significantly reduced at the linac exit (curve 2, Fig. 1). With existing instrumentation, we cannot accurately measure the actual loss of the targeted state in the course of beam acceleration in the linac. Typically, the $^{124}Xe^{28+}$ ion intensity corresponds to $5 \cdot 10^7$ ions at HILAC exit with total beam pulse duration of about 12-15 μs.
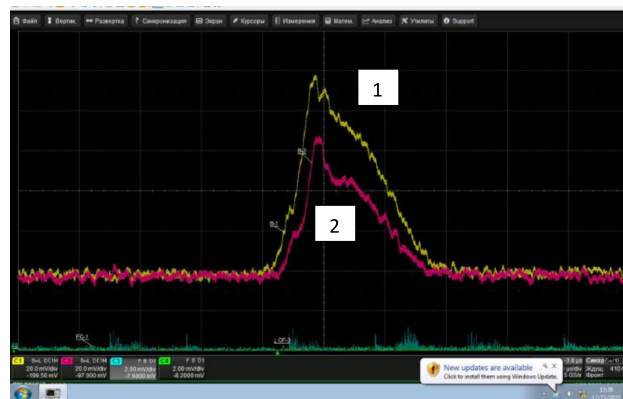
Figure1: Signals of current transformers at the RFQ exit (curve 1) and the HILAC exit (curve 2).

Curve 1 in Fig. 2 presents a typical magnetic cycle of the Booster. As one can see from curve 2, showing the beam current, the beam is injected at the first plateau, where it is adiabatically bunched at the 5th harmonic. Then the beam is accelerated to the second plateau corresponding the ion energy of 65 MeV/u, where it is adiabatically rebunched to the first harmonic. Finally, the beam is accelerated to the top energy of 205 MeV/u and extracted to Nuclotron. Typically, the accelerated to top energy $^{124}Xe^{28+}$ ions constitute about 60% of all ions at the linac exit.

Note that the electron cooling installations are important part of the accelerating complex. The first one is already installed and operates in Booster, and two others will be installed in each of the collider rings.

The intensity the of Xe^{28+} ion beam is expected to increase by a factor of 2 during next Booster Run. However,

---

† valebedev@jinr.ru

EXPERIMENTS ON ELECTRON COOLING AND INTENSE SPACE-CHARGE AT IOTA

N. Banerjee*, G. Stancari, Fermilab, Batavia, Illinois, USA

M.K. Bossard, J. Brandt, Y-K. Kim, The University of Chicago, Illinois, USA

S. Nagaitsev, Thomas Jefferson National Accelerator Facility, Newport News, Virginia, USA

Abstract

The Integrable Optics Test Accelerator at Fermilab will explore beam dynamics in a ring with intense space-charge using 2.5 MeV proton beams with an incoherent tune shift approaching −0.5. We will use this machine to explore the interplay between electron cooling, intense space-charge, and coherent instabilities. In this contribution, we describe the machine setup including the design of the electron cooler and the lattice, list specific experiments and discuss the results of numerical simulations which include the effects of electron cooling and transverse space-charge forces.

INTRODUCTION

The grand challenges facing the accelerator and beam physics community include creating and sustaining beams with intensity and phase-space density an order of magnitude higher than what is achievable today [1]. In the realm of hadron storage rings, such gains are crucial for future proton drivers for neutrino generation [2], neutron sources [3] and muon colliders [4], along with heavy ion colliders for particle and nuclear physics. Specifically at Fermilab, the Accelerator Complex Evolution plan [5], which aims to provide substantially more protons on target when compared to PIP-II [6], requires the replacement of the Fermilab Booster [7] synchrotron. One class of options involves constructing a rapid cycling synchrotron which will operate at high intensity and high space-charge tune shift to sustain 2.4 MW beam power on the Long-Baseline Neutrino Facility (LBNF) target. The Integrable Optics Test Accelerator (IOTA) [8], displayed in Fig. 1, was constructed at Fermilab as part of the R&D program toward achieving multi-megawatt proton beams. Research at IOTA includes Non-linear Integrable Optics [9,10], coherent instabilities, beam cooling [11], electron lenses [12], and more [13, 14]. IOTA was designed to operate both with 150 MeV electrons, which we have been using until now, and also 2.5 MeV protons, whose injector we are building. The proton program in IOTA is designed for experiments up to an incoherent tune shift of −0.5 to explore methods of improving the stability of bright and intense hadron beams in synchrotrons and storage rings.

The primary mechanism through which space-charge affects beam dynamics in hadron storage rings is through betatron resonance excitations [15] due to incoherent tune shifts of the particles as a function of position inside the bunch. In practice, periodic resonance crossing [16] of particles undergoing synchrotron motion in bunched beams lead to
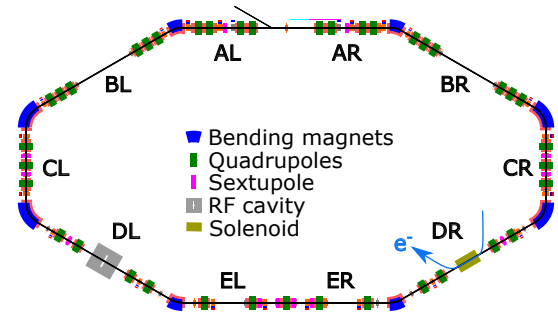
Figure 1: Layout of the Integrable Optics Test Accelerator [8] without special non-linear magnets. The beam moves clockwise. The blue arrow indicates the propagation of electrons in the cooler situated in section DR.

emittance growth and beam loss, thus limiting the maximum phase-space density which can be sustained in a ring. Studying these effects in high-energy hadron rings is complicated since the tune spread generated by space-charge dynamically changes the phase-space distribution of the bunch, which in turn influences the tune shift itself. Consequently, by using an electron cooler to enforce an equilibrium phase-space distribution in the bunch core, we can measure halo formation and beam loss in the presence of almost constant space-charge forces. Past experiments using electron cooling, seeking to maximize the Laslett tune shift of accumulated beam, found an upper limit of $|\Delta \nu_\perp| \sim 0.1 - 0.2$ [17, 18]. Using magnetized electron cooling of 2.5 MeV proton beams in IOTA, we seek to maximize the phase-space density of stored beam, measure beam loss and characterize the distribution.

While space charge restricts the maximum phase-space density of the beam, the onset of coherent excitations, such as the Transverse Mode Coupling Instability (TMCI), constrains the maximum current. In contrast, incoherent particle motion in the bunch with different betatron tunes results in Landau damping, which naturally restricts the growth of these instabilities. We can exploit this effect by providing non-linear focusing to the beam using octupoles [19] or electron lenses [20], and this has been instrumental in boosting the beam current in many accelerators. However, strong non-linear focusing also restricts the dynamic aperture, which constrains the maximum phase-space volume occupied by the bunch. We will explore Non-linear Integrable Optics (NIO) [21, 22] at IOTA, which can produce adjustable tune spread while ensuring stable single-particle dynamics where theoretically, the aperture is solely limited by the vacuum

---

* nilanjan@fnal.gov